ARL-AERO-PROP-TM-437

AR-004-488

DEPARTMENT OF DEFENCE

DEFENCE SCIENCE AND TECHNOLOGY ORGANISATION

AERONAUTICAL RESEARCH LABORATORIES

MELBOURNE, VICTORIA

Aero Propulsion Technical Memorandum 437

INTERPOLATION TECHNIQUES FOR THE TIME DOMAIN AVERAGING OF VIBRATION DATA WITH APPLICATION TO HELICOPTER GEARBOX MONITORING

by

P.D. McFADDEN

Approved for Public Release

SEPTEMBER 1986

AR-004-488

DEPARTMENT OF DEFENCE
DEFENCE SCIENCE AND TECHNOLOGY ORGANISATION
AERONAUTICAL RESEARCH LABORATORIES

Aero Propulsion Technical Memorandum 437

INTERPOLATION TECHNIQUES FOR THE TIME DOMAIN AVERAGING OF VIBRATION DATA WITH APPLICATION TO HELICOPTER GEARBOX MONITORING

by

P.D.McFadden

SUMMARY

Interpolation techniques provide an alternative to the phase-locked frequency multiplier for the calculation of the time domain average of a vibration signal. Higher order interpolation techniques produce flatter passbands and lover sidelobes in the stopband but require longer calculation times. Aliasing errors are introduced into the result by replication of the sidelobes during interpolation. In general, the errors are attenuated by time domain averaging, but under some conditions may be passed without attenuation.

POSTAL ADDRESS: Director, Aeronautical Research Laboratories,
P.O. Box 4331, Melbourne, Victoria 3001, Australia.

CONTENTS

1. INTRODUCTION

Time domain averaging is a signal processing technique which permits the extraction of periodic waveforms from noisy signals. It is particularly useful for the analysis of the vibration of mechanical systems such as gearboxes, as it enables the vibration of a single gear to be separated from the vibration of the complete system. As the vibration of the gear is shown in the time domain over one complete revolution, differences in the performance of the teeth around the gear become apparent, enabling faults such as fatigue cracks to be identified. Recently, time domain averaging has been applied with considerable success to the detection of fatigue cracks in the input spiral bevel pinion in the main rotor gearbox of the Wessex helicopter [1].

Time domain averaging differs from the conventional technique of spectral analysis in that it requires a rotational reference signal to enable the angular position of the desired gear in the system to be determined. In its simplest form, this reference signal may consist of a pulse train which is synchronized with the rotation of the required gear. This pulse train may be used to control the sampling of the vibration signal. However, the acquisition of a signal directly from the required gear or its shaft is often not practicable as these components may not be readily accessible. In such cases, it is necessary to take a reference signal from some other location in the system which is readily accessible, and to convert that signal to the required sampling control signal using a phase-locked frequency multiplier. For the analysis of the vibration of the Wessex input pinion, a simple phase-locked frequency multiplier was developed to convert the alternator output waveform, at a nominal 400 Hz, into a pulse train which provides 256 samples per revolution of the pinion [2].

But the phase-locked frequency multiplier is not without its own problems. In the phase-locked frequency multiplier developed for the Wessex pinion, an edge-triggered digital phase detector was used. It has been found on some occasions that this is susceptible to false triggering by electrical noise on the alternator signal or dropouts on the tape recording, causing the loop to lose lock and so corrupt the time domain average. Furthermore, in order to optimize the performance of the phase-locked frequency multiplier for any given application, it is necessary to select the loop filter characteristics to suit the expected input frequency and the multiplication ratio of the loop. Changing the multiplication ratio to enable the time domain averaging of different gears in the system requires the changing of the loop filter and, for a multi-stage multiplier, this adds greatly to the complexity of the design. Furthermore, the phase-locked loop requires a finite time to acquire and lock onto the input signal. Under some circumstances this time can be very large, necessitating long recordings of the data of which only a small part can actually be used when the loop has finally locked. Even when locked, the loop must inevitably lag behind any changes in the phase or frequency of the input signal, and these errors must limit the accuracy of the average which is obtained.

As an alternative to the phase-locked frequency multiplier, a technique for time domain averaging based on off-line interpolation by a

digital computer can be employed. If both the vibration signal and the rotational reference signal are sampled simultaneously at a fixed clock frequency, then for each sample of the vibration signal the corresponding rotational reference position will also be known. From the numbers of teeth on the gears in the system, the reference signal can be related to the rotation of the required gear, and the vibration signal can then be interpolated to obtain the vibration of the system at increments of the rotation of the required gear. From these values the time domain average may be calculated.

This technique has several advantages over the phase-locked frequency multiplier. Firstly, the sensitivity to noise on the reference signal is reduced, as it is possible to process the sampled reference signal to remove some of the interference. As all of the processing is performed off-line, more time is available for such operations than if on-line averaging is attempted. Secondly, only one complete cycle of the reference signal is required before the technique can start producing interpolated data, unlike the phase-locked frequency multiplier which may require many cycles before lock can be achieved. Thus many more averages can be obtained from the same quantity of data. But the biggest advantage promises to be the ease of changing the multiplication ratio. With the phase-locked frequency multiplier this required the changing of loop filters, but with the interpolation technique it can be achieved in a computer program simply by changing the ratio relating the rotation of the required gear to the reference signal. In principle, this makes possible the calculation of the time domain average of any gear in a mechanical system.

It is believed that a linear interpolation technique may already have been used for the time domain averaging of gear vibration. Linear interpolation is very simple to implement, but the results it produces are only approximate. It is very important that interpolation techniques, as they may be applied to time domain averaging, should be understood from a digital signal processing viewpoint, in order that the frequency response of the techniques may be estimated and that parameters may be selected to optimize the performance of the techniques. This report examines the theory of interpolation as applied to time domain averaging and describes the sample and hold, linear and cubic interpolation techniques, comparing the frequency response of each. It is revealed that interpolation techniques introduce aliasing errors which produce images of spectral components at other frequencies. It is shown that while linear interpolation can be satisfactory, cubic interpolation provides greater accuracy as it has a better frequency response and reduced aliasing errors, although it does require a longer calculation time. The techniques are illustrated by examples relevant to the analysis of the vibration of the input spiral bevel pinion in the main rotor gearbox of the Wessex helicopter.

2. FREQUENCY RESPONSES OF INTERPOLATION TECHNIQUES

Sample and hold interpolation, also known as zero order hold, is the simplest interpolation technique. The incoming signal $x(t)$ is sampled and the value obtained is held until the next sample has been taken, after which that new value is held, and so on. To evaluate the frequency response of the sample and hold interpolation, the technique is expressed

in terms of simple digital signal processing operations. Firstly, the incoming signal is sampled at a frequency f_s by multiplying the signal by a train s(t) of unit impulses with period $T_s=1/f_s$, as illustrated in Figure 1a. By the convolution theorem [3], multiplication in the time domain is equivalent to convolution in the frequency domain. Thus in the frequency domain, the Fourier transform X(f) of the signal is convolved with the Fourier transform S(f) of the train of impulses, which is also a train of impulses but at multiples of the sampling frequency f_s. This produces replicates of the original baseband at multiples of the sampling frequency, as shown in Figure 1b. The result is then convolved with a rectangle function a(t) of width T_s and amplitude 1, as illustrated in Figure 2a. By the convolution theorem [3], convolution of signals in the time domain is equivalent in the frequency domain to the multiplication of the Fourier transforms of those signals, producing the result shown in Figure 2b. When interpolation is performed and the Fourier transform A(f) of the rectangle function is multiplied by the Fourier transform of the sampled signal, the replicates must be included in the latter. Parts of the replicates may be passed by the sidelobes in the Fourier transform of the rectangle function, although at reduced amplitude.

The rectangular function a(t) may be defined by:

$$\begin{aligned} a(t) &= 1 \quad \text{for } 0 < t < T_s \\ &= \tfrac{1}{2} \quad \text{for } t = 0,\ t = T_s \\ &= 0 \quad \text{elsewhere} \end{aligned} \tag{1}$$

Its Fourier transform A(f) is given by:

$$\begin{aligned} A(f) &= (\sin(\pi T_s f)/\pi f)\ e^{-j2\pi f(T_s/2)} \\ &= T_s\ (\sin(\pi T_s f)/(\pi T_s f))\ e^{-j2\pi f(T_s/2)} \end{aligned} \tag{2}$$

Note the presence in the above equation of the sidelobes which decrease inversely with the frequency. Note also the non-zero phase characteristic, which is due to the holding of the previous sample value, thereby introducing a time delay of $T_s/2$ into the result. A simpler presentation of interpolation has been presented [4], but it is incorrect as it neglects the replication in the frequency domain caused by the sampling of the signal.

Linear interpolation, also known as first order hold, is another simple interpolation technique. After sampling the signal, the required intermediate values are obtained by linear interpolation between the samples either side of the required abscissa. To evaluate the frequency response of linear interpolation, the technique is expressed in terms of simple digital signal processing operations. Firstly, the incoming signal is sampled as for the sample and hold interpolation. Then the sampled signal is convolved with a triangular function b(t) of width $2T_s$ and amplitude 1, as shown in Figure 3a. In the frequency domain, the Fourier transform of the sampled signal is multiplied by the Fourier transform B(f)

of the triangular function, as illustrated in Figure 3b. Parts of the replicates of the baseband may be passed by the sidelobes of the latter, as for the sample and hold interpolation, but as the sidelobes of the triangular function are smaller than those of the rectangular function, the amount passed should be smaller.

The triangular function b(t) may be defined by:

$$\begin{aligned} b(t) &= 1 - t/T_s \quad \text{for } |t| < T_s \\ &= 0 \qquad\quad \text{elsewhere} \end{aligned} \tag{3}$$

Its Fourier transform B(f) is given by:

$$\begin{aligned} B(f) &= \sin^2(\pi T_s f)/(\pi f)^2 T_s \\ &= T_s\,(\sin(\pi T_s f)/(\pi T_s f))^2 \end{aligned} \tag{4}$$

Note the presence in the above equation of the sidelobes which decrease inversely with the square of the frequency, more rapidly than for the rectangular function. Unlike the sample and hold interpolation, the phase characteristic is zero, as no time delay is introduced.

For better performance, a more sophisticated interpolation technique such as cubic interpolation, also known as third order hold, is a logical choice. Whereas linear interpolation utilized a single sample either side of the required abscissa, cubic interpolation uses two samples either side. A cubic function may be fitted simply to four samples by the Lagrangian interpolation formula of order four [5]. To evaluate the frequency response, the interpolation is expressed in terms of simple digital signal processing operations. Firstly, the incoming signal is sampled as for the sample and hold and linear interpolations. Then the sampled signal is convolved with the impulse response c(t) of the cubic function, having a width $4T_s$ and amplitude 1, as shown in Figure 4a. In the frequency domain, the Fourier transform of the sampled signal is multiplied by the Fourier transform C(f) of the cubic function, as illustrated in Figure 4b. Parts of the replicates of the baseband may be passed by the sidelobes of the cubic function, but as these are very much smaller than those of either the sample and hold or linear interpolation functions, the signal passed by the sidelobes will be correspondingly smaller. Unlike the sample and hold and linear interpolation techniques for which the determination of the impulse response was easy, for cubic interpolation it is rather more difficult, and the impulse response is different depending on where the four samples are placed relative to the required abscissa. Only the case in which two samples are located either side of the required value will be considered here. Techniques for calculating the impulse response of Lagrangian interpolation functions have already been described [6]. Using these techniques, the impulse response c(t) for Lagrangian interpolation of order four is found to be:

$$\begin{aligned} c(t) &= H_2(t/T_s + 2) \quad \text{for } -2T_s < t \leq -T_s \\ &= H_1(t/T_s + 1) \quad \text{for } -T_s < t \leq 0 \end{aligned}$$

$$= H_0(t/T_s) \quad \text{for} \quad 0 < t \leq T_s$$

$$= H_{-1}(t/T_s - 1) \quad \text{for} \quad T_s < t \leq 2T_s \tag{5}$$

where

$$H_2(v) = (v + 1)(v)(v - 1)/6$$

$$H_1(v) = -(v + 1)(v)(v - 2)/2$$

$$H_0(v) = (v + 1)(v - 1)(v - 2)/2$$

$$H_{-1}(v) = -(v)(v - 1)(v - 2)/6 \tag{6}$$

The Fourier transform C(f) is found to be:

$$C(f) = T_s\,(1 + (2\pi T_s f)^2/6)\,(\sin(\pi T_s f)/(\pi T_s f))^4 \tag{7}$$

Note in the above equation the presence of the sidelobes which, for large frequencies, decrease inversely with the square (not the fourth power) of the frequency. The sidelobes will be smaller than for the linear interpolation due to the fourth power of the sine term. The phase characteristic is zero as no time delay is introduced.

The frequency responses of the sample and hold, linear and cubic interpolation techniques are compared in Figure 5. Increasing the order of the interpolation technique decreases the amplitude of the sidelobes, so producing better stopband performance. The cubic function produces a flatter passband than either the sample and hold or linear functions, and also has the sharpest cutoff rate. Thus the cubic function clearly provides better frequency response, although the higher order must increase the calculation time.

3. ALIASING ERRORS PRODUCED BY INTERPOLATION

In the previous section, interpolation techniques were introduced and their effects in the time and frequency domains were demonstrated. However, the results produced were continuous functions and not discrete samples, even though the original signal had been sampled. The interpolated results obviously cannot be used in this form, as a digital computer can only operate on discrete values. These could be created by sampling the interpolated signals, although in practice this would not normally be done, as the interpolation function need be evaluated only at the required abscissa, thus reducing the time required for computation. However, to simplify the analysis, the evaluation will be modelled as a sampling process.

The interpolated signal is sampled as shown in Figure 6a by multiplying it by a train u(t) of unit impulses with a period T_I, where in general $T_I \neq T_s$. From the convolution theorem, multiplication in the time

domain is equivalent to convolution in the frequency domain. Thus the Fourier transform of the interpolated signal is convolved with the Fourier transform U(f) of the train of impulses, which is also a train of impulses at multiples of the interpolation frequency $f_I=1/T_I$, as illustrated in Figure 6b. A particularly important results becomes apparent. The sidelobes which are present in the continuous, interpolated signal are replicated during the convolution and may overlap the baseband and stopband, so producing errors in the result. These errors will be referred to here as aliasing errors, because the image of a signal is made to appear at a different frequency. These aliasing errors should not be confused with the more common use of the term to describe errors which are produced by the sampling of a signal at an insufficient rate.

The magnitude of the aliasing errors depends on three factors. Firstly, it depends on the magnitude of the sidelobes present in the frequency response of the interpolation function, and secondly the separation of the replicates, which is determined by f_I, and thirdly by the bandwidth of the original signal. The smaller the sidelobes and the signal bandwidth and the larger the interpolation frequency then the lower will be the interference between the sidelobes and the main lobe. Reducing the sidelobes requires the use of more sophisticated interpolation techniques. Increasing the interpolation frequency requires more frequent evaluation of the interpolation function. Both will increase the time taken to calculate the result. Reducing the bandwidth limits the usefulness of the result. A compromise solution is required which combines acceptable levels of aliasing errors with acceptable calculation time.

In order to demonstrate the effects of aliasing errors, an example will be presented which is relevant to the analysis of the vibration of the input spiral bevel pinion in the Wessex helicopter main rotor gearbox. The pinion rotates at a nominal frequency of 43 Hz, while the alternator signal, nominally 400 Hz, is used as the rotational reference signal. The frequency of the gear rotation f_R is related to the alternator frequency f_A by the numbers of teeth on the gears and the number of poles in the alternator. After elimination of common factors, this is given by [2]:

$$f_R = (19/61) \times (21/61)\, f_A \qquad (8)$$

The first example features test signals synthesized as follows. The alternator signal is modelled as a sinusoid of unit amplitude and frequency f_A=401.57 Hz. The vibration signal is the sum of 128 sinusoids of unit amplitude at frequencies from 1 to 128 times f_R in increments of f_R. Both are evaluated at intervals corresponding to a sampling rate f_S=20480 Hz and stored in blocks of 512 sample pairs on disc. The value of f_A was chosen to produce exactly 51 samples per simulated alternator cycle. Hence for the test signal:

$$f_S = 51\, f_A \qquad (9)$$

Applying the sample and hold interpolation technique to the test signal and sampling the result at a frequency $f_I=1024f_R$ produces a signal having the amplitude spectrum shown in Figure 7. Many aliasing errors are visible, with the largest of these occurring at about 350 orders due to the first

upper sidelobe of the baseband. Other major features can also be identified as sidelobes of replicates. Some even overlap the baseband and interfere with signal in the band of interest between 1 and 128 orders. Using linear interpolation of the same data, the spectrum in Figure 8 is produced, with greatly reduced aliasing errors in both the passband and stopband. Using cubic interpolation, the spectrum in Figure 9 is produced, with further reductions in aliasing errors.

4. EFFECT OF TIME DOMAIN AVERAGING ON ALIASING ERRORS

In the previous section, the effects of sampling the interpolated signals were demonstrated. A key feature was the introduction of aliasing errors by the replication of sidelobes falling within the passband and stopband. For sample and hold and linear interpolation, these errors were significant. Fortunately, with many signals time domain averaging can help to reduce these errors. Averaging is performed using the interpolated signal evaluated at f_I where f_I is an integer multiple of the rotation frequency f_R of the required gear. That is, $f_I=Lf_R$ where L is an integer. The original sampling frequency f_S is selected from the sampling rates which are available on the data acquisition system, and as this is in general independent of the rotation frequency of the mechanical system, f_S and f_I will in general be independent. All of the components passed by the time domain averaging process will be at multiples of the rotation frequency f_R, and as $f_I=Lf_R$, all of the components in the replicates of the baseband will be at multiples of f_R. However, aliased images of these, present in all of the sidelobes, will not in general be at multiples of f_R.

For example, consider the first sidelobes of the baseband produced by the sampling of the original signal at f_S. A component in the baseband at a frequency $f_M=Mf_R$, where M is an integer, will be passed by time domain averaging. Its aliased image in the first sidelobe will appear at f_S+f_M, which will not in general be an integer multiple of f_R, and so after averaging the image will be attenuated. Similarly, for the first lower sideband of the first replicate of the baseband, the aliased image will be located at $f_I-f_S-f_M$, which in general will not be an integer multiple of f_R, and so with averaging will be attenuated. The effects of averaging on aliasing errors will be demonstrated using the test signal described in the previous section. The amplitude spectrum of the signal obtained after 128 averages using sample and hold interpolation is shown in Figure 10There is a marked improvement over that shown in Figure 7 as the passband is now smooth and the aliasing errors in the stopband have been attenuated. For linear interpolation, the result is seen in Figure 11, and similarly for cubic interpolation in Figure 123.

In general, time domain averaging tends to attenuate aliasing errors which are generated by interpolation, but there are specific instances in which aliasing errors will not be reduced. For example, consider an unwanted periodic noise at a frequency f_N, such as might be generated by another gear meshing frequency, with $f_N \neq Nf_R$ where N is an integer. Thus in the baseband, f_N will be attenuated. However, sampling of the signal at a frequency f_s produces replication of the Fourier transform about f_S, so that an image of f_N appears at $f_S \pm f_N$. After averaging, the image at f_S-f_N will remain if:

$$f_S - f_N = Kf_R \quad \text{where K is an integer} \tag{10}$$

If K=350, then from Equations 8,9 and 10, $f_N=125.62f_R$. Thus a periodic noise signal occurring at 125.62 orders will produce an aliased image at 350 orders which will be attenuated by the filter shape of the interpolation function, but will not be attenuated further by time domain averaging.

This is illustrated by comparing the spectra obtained after 1 and 128 averages of a test signal synthesized featuring a periodic component at a frequency of 125.62 orders. With sample and hold interpolation, the spectrum after a single average in Figure 13 shows many images, with the biggest consisting of a peak near 126 orders surrounded by many sidebands, but with a clean peak at 350 orders. After 128 averages, the peak at 350 orders remains unchanged in amplitude while all other components are attenuated, as shown in Figure 14. For linear interpolation, after a single average there are fewer images as illustrated in Figure 15, with the largest peak occurring again near 126 orders and a clean peak at 350 orders having a lower amplitude than before due to the smaller sidelobes. After 128 averages, the peak at 350 orders remains unchanged in amplitude while all other components are attenuated, as shown in Figure 16. For cubic interpolation, after a single average there are even fewer images as illustrated in Figure 17. After 128 averages, the peak at 350 orders remains unchanged as shown in Figure 18. This demonstrates the importance of the amplitude of the sidelobes in suppressing this class of aliasing error.

Errors can also be produced in the passband. For example, images can be produced in the second lower sidelobe of the replicate about f_I such that:

$$f_I - 2f_S + f_N = Kf_R \quad \text{where K is an integer} \tag{11}$$

If K=120, then from Equations 8,9 and 11 with $f_I=1024f_R$, $f_N=47.33f_R$. Thus a periodic noise component at 47.33 orders will produce an image at 120 orders. The image will be attenuated by the filter shape of the interpolation function but will not be attenuated further by averaging.

This is demonstrated for 1 and 128 averages for a test signal synthesized with a periodic signal at 47.33 orders. With sample and hold interpolation, after a single average many images are produced as shown in Figure 19. The biggest peak occurs near 47 orders surrounded by many sidebands, but with a clean peak at 120 orders. After 128 averages, as shown in Figure 20, the peak at 120 orders remains unchanged in amplitude, while the components near 47 orders are heavily attenuated. With linear interpolation, after a single average no images can be seen on the original scale, only the major peak near 47 orders, as illustrated in Figure 21. After 128 averages, Figure 22 shows on an enlarged scale that there is a small component present at 120 orders, together with the remains of the peak near 47 orders which has not yet been completely attenuated. For cubic interpolation, no images can be seen on the original scale in Figure 23, only the major peak near 47 orders. After 128 averages, Figure 24 shows on an enlarged scale that there is a very small component present at 120 orders, together with the remains of the peak near 47 orders. This demonstrates that aliasing errors can be produced in the passband which may

not be completely attenuated by time domain averaging. The more sophisticated interpolation schemes, having better stopband performance, help to reduce the amplitude of these errors.

The examples considered so far have assumed that the rotation frequency f_R is exactly constant. This is unlikely to occur in practice, particularly in helicopter gearboxes for which speed variations of up to ±1 % might be expected at a nominally constant torque setting. These small speed or frequency variations will be referred to as jitter. Synchronous noise at a frequency f_N will vary directly with variations in the rotation reference frequency f_A. The interpolation frequency f_I will also vary directly with f_R since $f_I=Lf_R$, but the sampling frequency f_S remains constant as it is fixed by the data acquisition equipment. Thus the equations developed previously to describe the images may not hold. That is, if $f_N=125.62f_R$, the aliased image will not remain steady at $350f_R$ as f_R and f_N vary. Similarly, if $f_N=47.33f_R$, the aliased image will not remain fixed at $120f_R$. As a result, the noise will be attenuated by time domain averaging. The extent of the attenuation will depend on the magnitude of the jitter. Although the worst case amplitude of the aliasing errors may be reduced, other periodic components may produce images for a short time, thus contributing to low level noise in the average. It is difficult to predict the amplitude of the aliasing errors without a knowledge of the possible periodic components and the frequency distribution of the rotation frequency f_R.

The examples considered so far have all been numerically generated. Now examine the calculation of the time domain average of the vibration of the Wessex input pinion in practice using sample and hold, linear and cubic interpolation. All examples are calculated using the same input data sampled and stored on disc by a separate program. Samples were taken at an effective rate of 20480 Hz per channel. The vibration signal was lowpass filtered at 4 kHz. The results after 512 averages are shown in Figure 25, 26 and 27. There is little visible difference. Previously a narrowband enhancement technique has been developed for analysis of the vibration of the Wessex pinion [1]. This technique can be applied to averages presented here by bandpass filtering in the range 8 to 36 orders inclusive and eliminating the meshing component at 22 orders, then enveloping and calculating the kurtosis. The results are shown in Table 1. For linear and cubic interpolation, the kurtosis values obtained differ by only 0.13 %, but the sample and hold interpolation differs from the others by more than 4.9 %. While this difference is not enough to affect the decision on the condition of the gear, it does indicate that measurable changes in the passband have occurred. Views of the spectra of the time domain averages are shown in Figures 28, 29 and 30, enlarged so as to reveal the components in the vicinity of the first sidelobe. The larger peaks in the spectra have amplitudes of approximately 10 g. For the sample and hold interpolation, the components in the sidelobe have amplitudes about 0.03 g present as a wideband noise across the spectrum, even intruding into the passband and so affecting the result. The best result is clearly obtained by cubic interpolation.

5. EXECUTION TIMES OF INTERPOLATION PROGRAMS

The execution times of programs running on a DEC LSI 11/73 under RT-11 Version 5 with Fortran IV using sample and hold, linear and cubic interpolation to process 128 averages of identical data are tabulated in Table 2. The cubic interpolation program requires more than twice the time needed for linear interpolation. Table 3 compares the execution times of the cubic interpolation program to process 100 averages of identical data when compiled under Fortran IV and Fortran 77. Clearly, the greater optimization of code performed by the latter compiler reduces the execution time by nearly one half.

6. MANIPULATION OF SPECTRUM

Since the time domain average is exactly periodic, the spectrum of the average is a pure line spectrum. By manipulating components in the frequency domain and then transforming back to the time domain, digital filtering can be performed to improve the passband and stopband shapes. For example, by setting the amplitudes of all the components at frequencies in the stopband to zero, the first sidelobe can be eliminated. Furthermore, if the passband is divided by the theoretical frequency response of the interpolation function, the passband can be made flat. However, setting of the stopband to zero will not remove aliasing errors from the passband, and dividing the passband can increase the amplitude of the aliasing errors there. Noise which is aliased into the passband cannot be eliminated by manipulation of the passband shape as a substitute for a good interpolation function.

7. CONCLUSIONS

Interpolation techniques provide an alternative to the phase-locked frequency multiplier for the calculation of the time domain average of a vibration signal when a rotational reference signal taken directly from the gear of interest is not available. The frequency response of the interpolation technique depends on the order of the technique used. Higher order techniques, such as Lagrangian cubic interpolation, have a flatter passband and smaller sidelobes in the stopband than simpler techniques such as sample and hold and linear interpolation. However, increasing the order of the interpolation technique also increases the time required for the calculation.

When the signal is interpolated at the new frequency, the baseband of the signal is replicated in the frequency domain at multiples of the new frequency. When sidelobes produced by the interpolation function are replicated into the original baseband, aliasing errors are introduced which corrupt the interpolated signal. In general, time domain averaging attenuates the aliasing errors, but under certain conditions, it is possible for noise signals to generate aliasing errors which will be passed by the time domain averaging process without attenuation. In practice, small fluctuations in the rotational speed of the mechanical system will assist the time time domain averaging to attenuate the aliasing errors. Nevertheless, the use of an interpolation technique of sufficiently high order is recommended to reduce the sidelobes and hence the aliasing errors.

REFERENCES

1. McFadden,P.D., "Analysis of the Vibration of the Input Bevel Pinion in RAN Wessex Helicopter Main Rotor Gearbox WAK143 Prior to Failure", Aeronautical Research Laboratories, Aero Propulsion Report 169, September 1985.

2. McFadden,P.D., "A Phase-Locked Frequency Multiplier for the Signal Averaging of the Vibration of the Wessex Helicopter Input Spiral Bevel Pinion", Aeronautical Research Laboratories, Aero Propulsion Technical Memorandum 423, January 1985.

3. Brigham,E.O., "The Fourier Transform", Prentice-Hall, New Jersey, 1974.

4. Oppenheim,A.V., Willsky,A.S. and Young,I.T., "Signals and Systems", Prentice-Hall, New Jersey, 1983, chapter 8.

5. Hildebrand,F.B., "Introduction to Numerical Analysis", McGraw-Hill, New York, 1956, chapter 3.

6. Schafer,R.W. and Rabiner,L.R., "A Digital Signal Processing Approach to Interpolation", Proceedings of the IEEE, Vol 61, no 6, pp 692-702, June 1973.

TABLE 1

Effect of Interpolation Scheme on Enhanced Signal

DEC LSI 11/73 RT-11 Wessex Input Pinion 512 averages

Interpolation Scheme	Kurtosis
Sample and Hold	3.149
Linear	3.001
Cubic	2.997

TABLE 2

Effect of Interpolation Scheme on Execution Time

DEC LSI 11/73 RT-11 Fortran IV 128 averages

Interpolation Scheme	Execution Time (s)
Sample and Hold	135
Linear	174
Cubic	431

TABLE 3

Effect of Compiler on Execution Time

DEC LSI 11/73 RT-11 Cubic Interpolation 100 averages

Compiler	Execution Time (s)
Fortran IV	337
Fortran 77	174

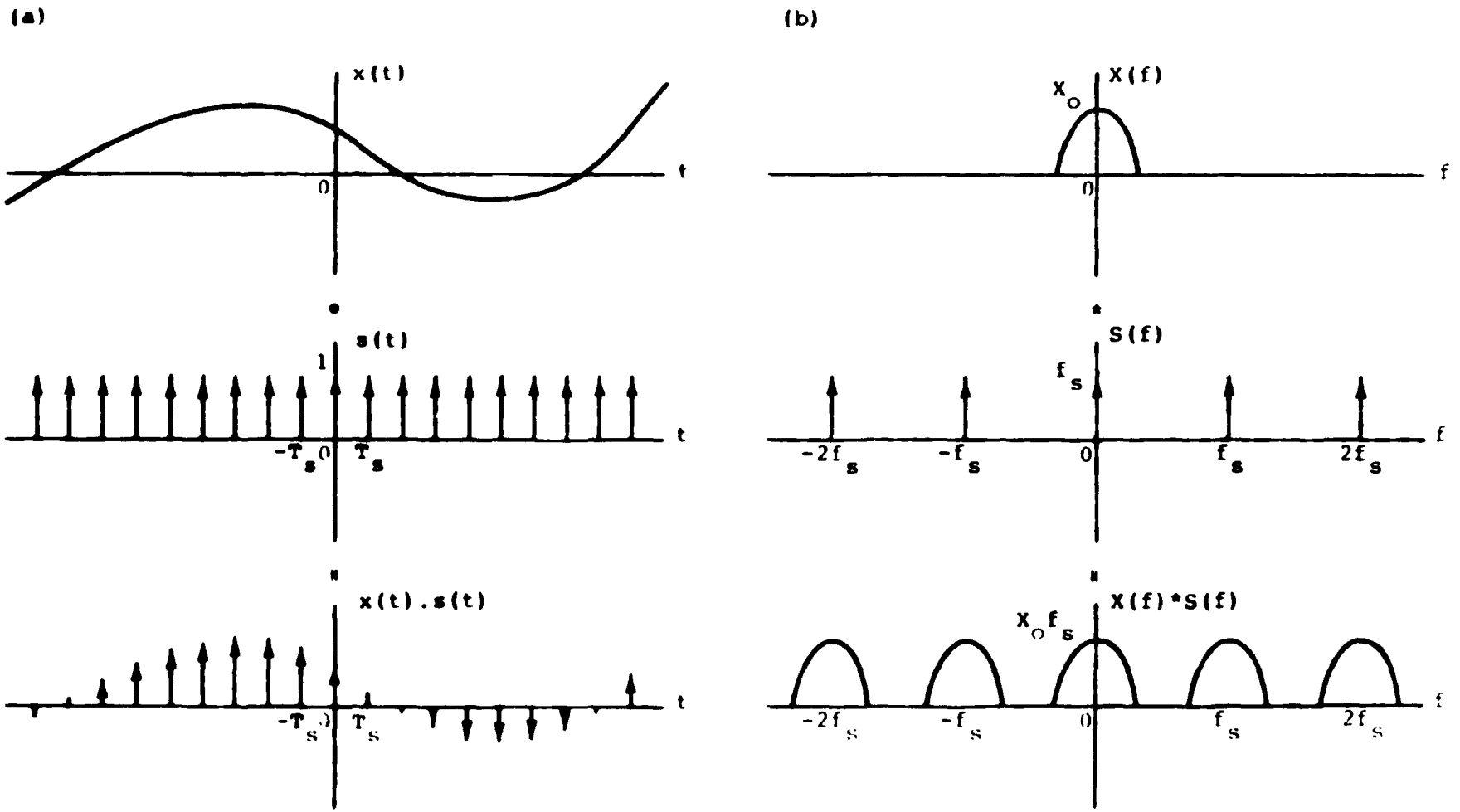

FIG. 1 SAMPLING OF INCOMING SIGNAL

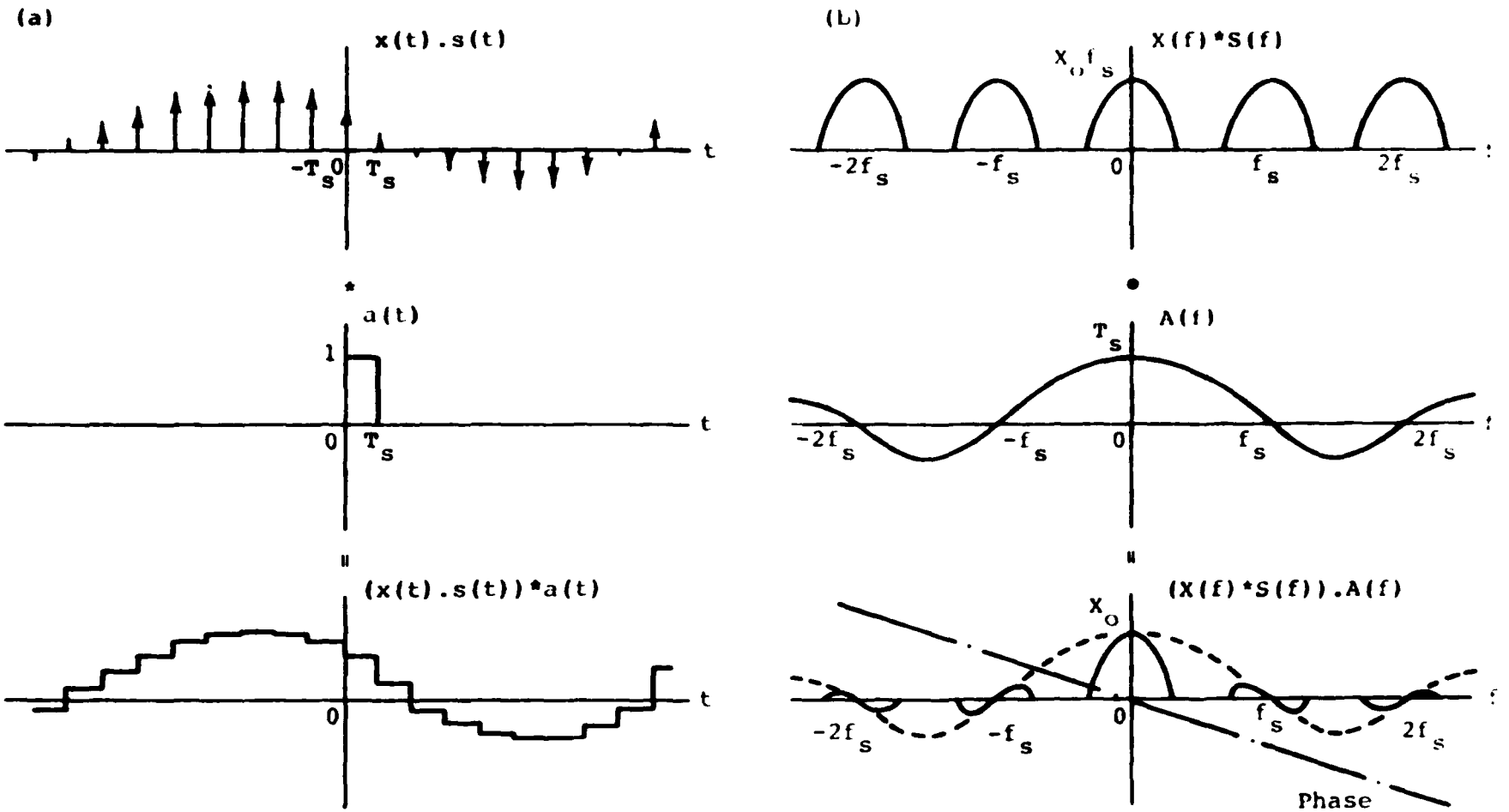

FIG. 2 SAMPLE AND HOLD INTERPOLATION OF SAMPLED SIGNAL

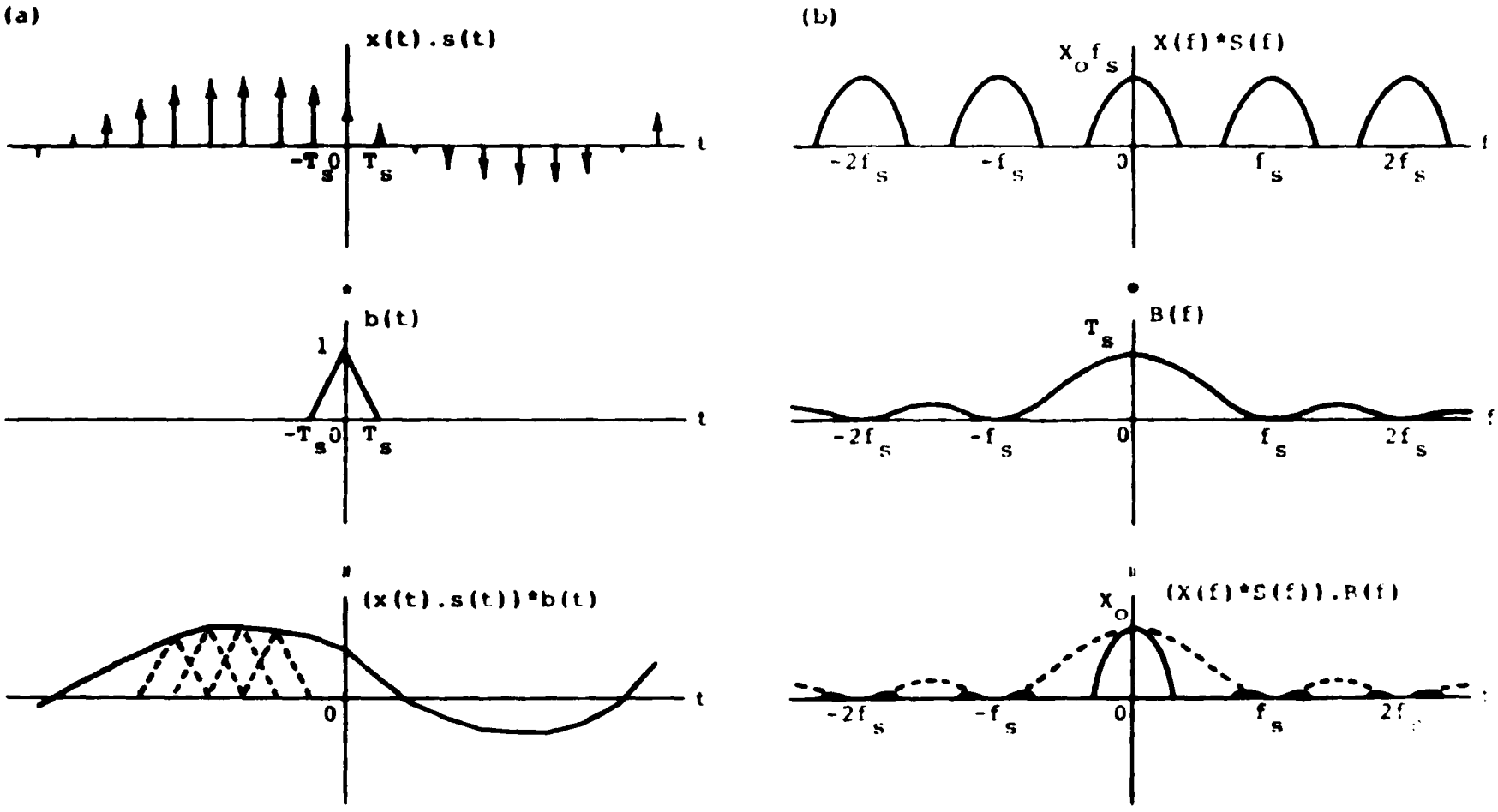

FIG. 3 LINEAR INTERPOLATION OF SAMPLED SIGNAL

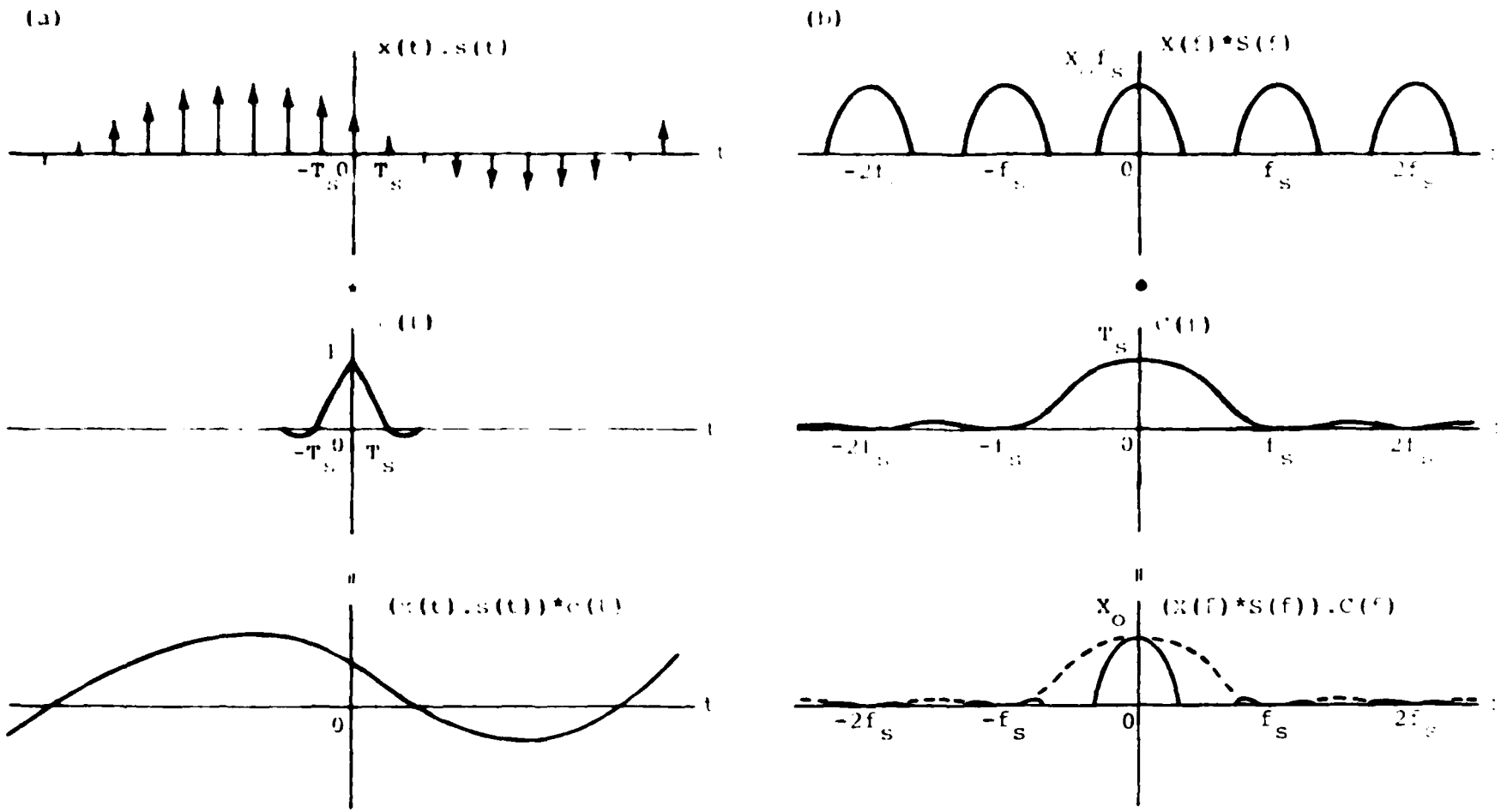

FIG. 4 CUBIC INTERPOLATION OF SAMPLED SIGNAL

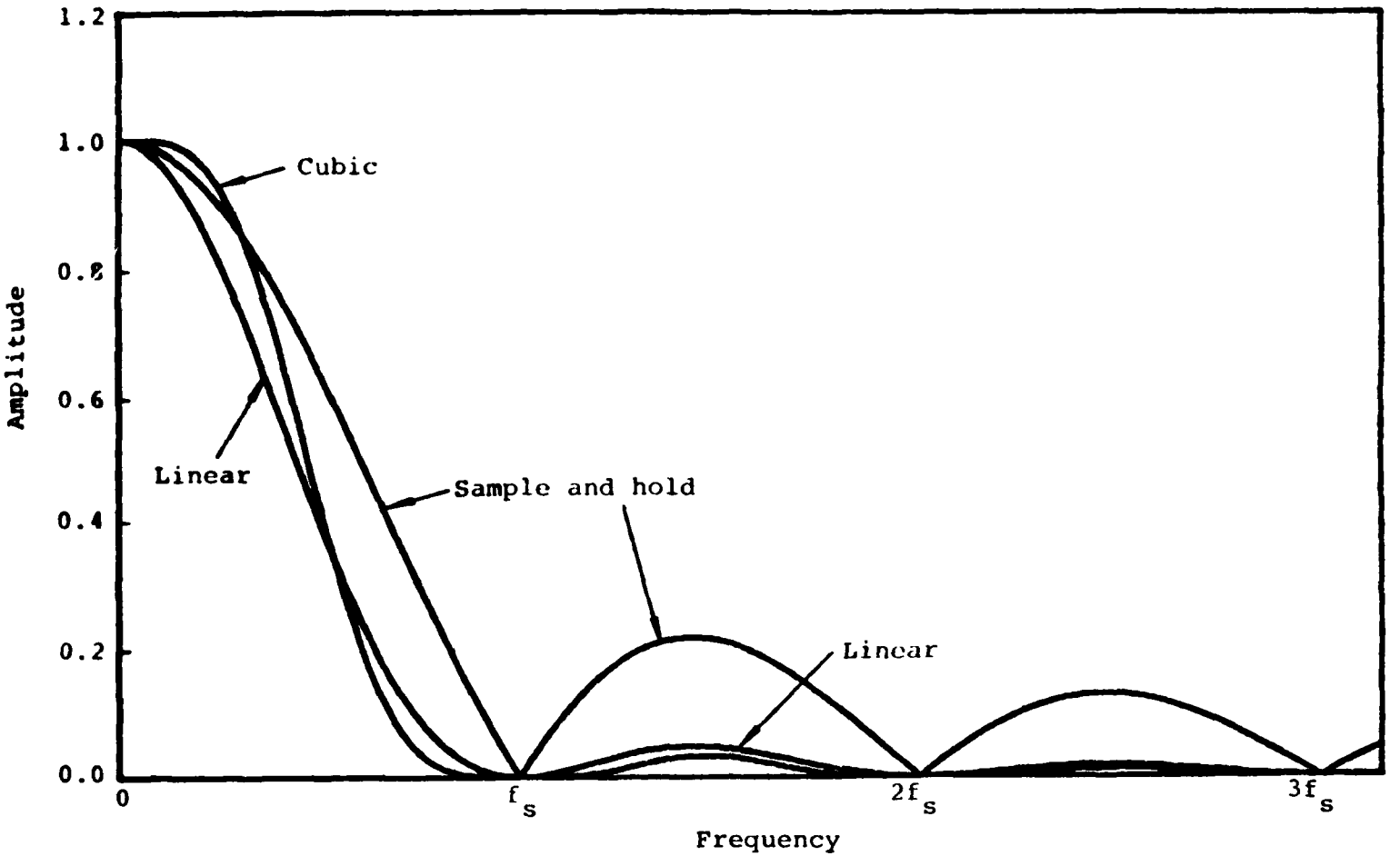

FIG. 5 COMPARISON OF FREQUENCY RESPONSES OF INTERPOLATION TECHNIQUES

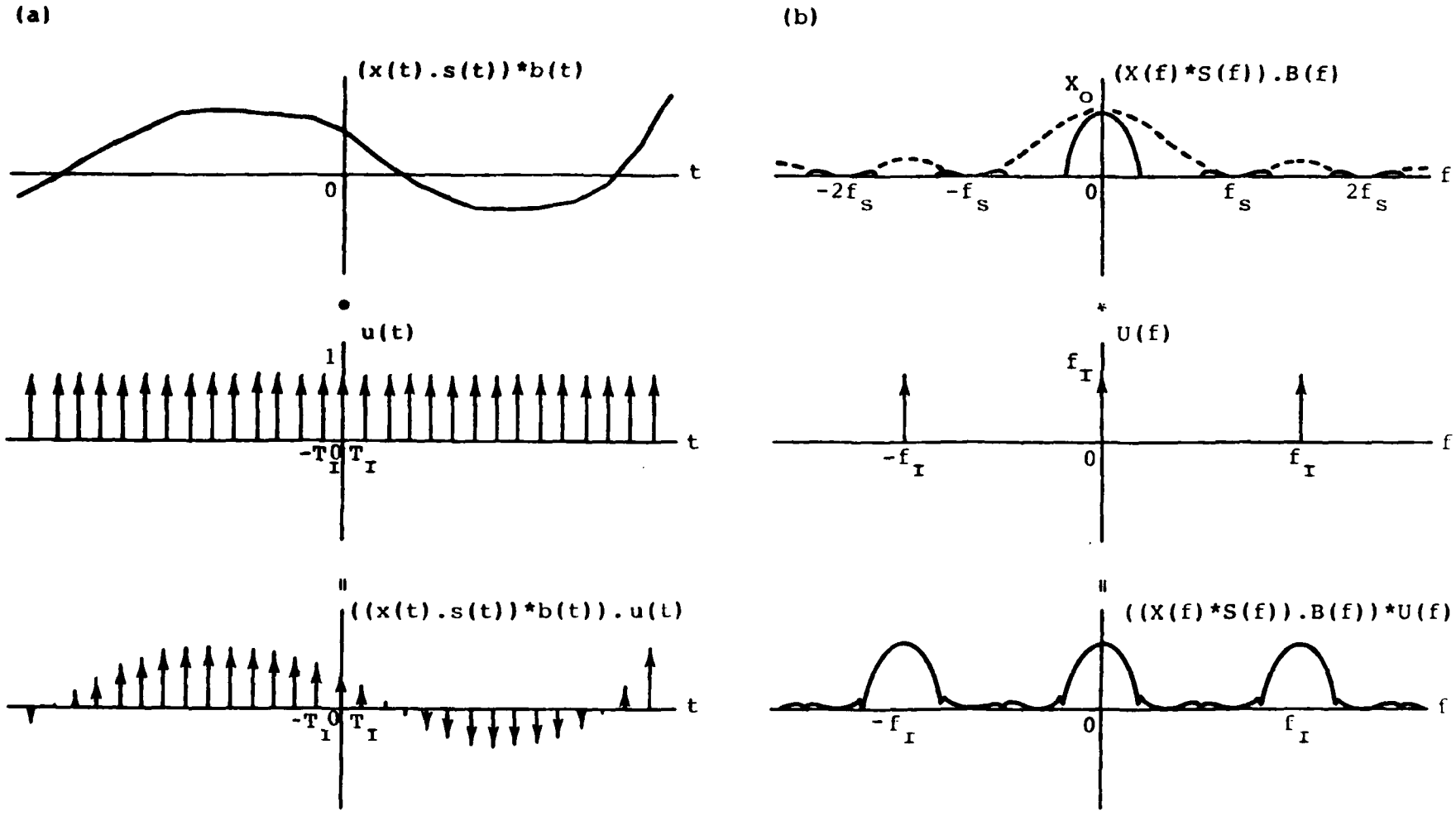

FIG. 6 SAMPLING OF LINEAR INTERPOLATED SIGNAL

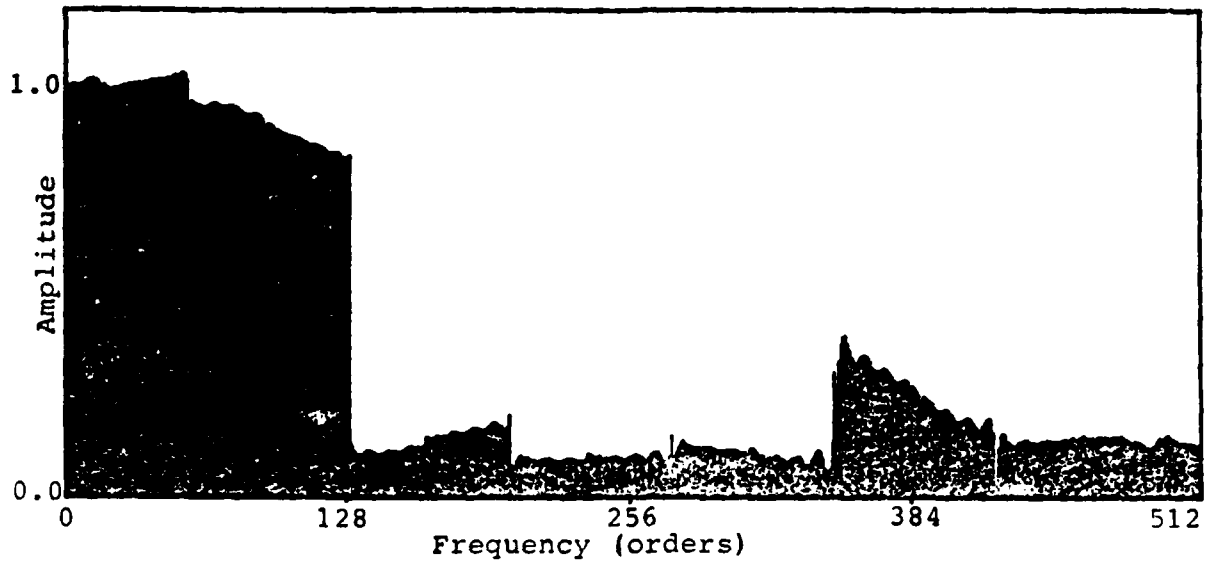

FIG. 7 AMPLITUDE SPECTRUM AFTER SAMPLE AND HOLD INTERPOLATION OF TEST SIGNAL 1 AVERAGE

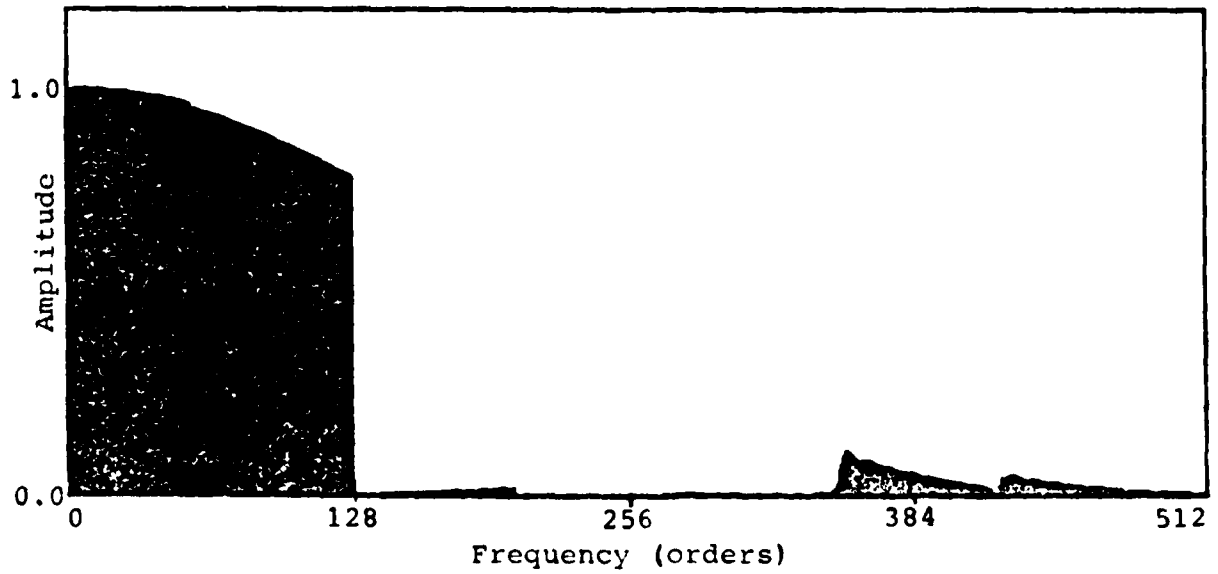

FIG. 8 AMPLITUDE SPECTRUM AFTER LINEAR INTERPOLATION OF TEST SIGNAL 1 AVERAGE

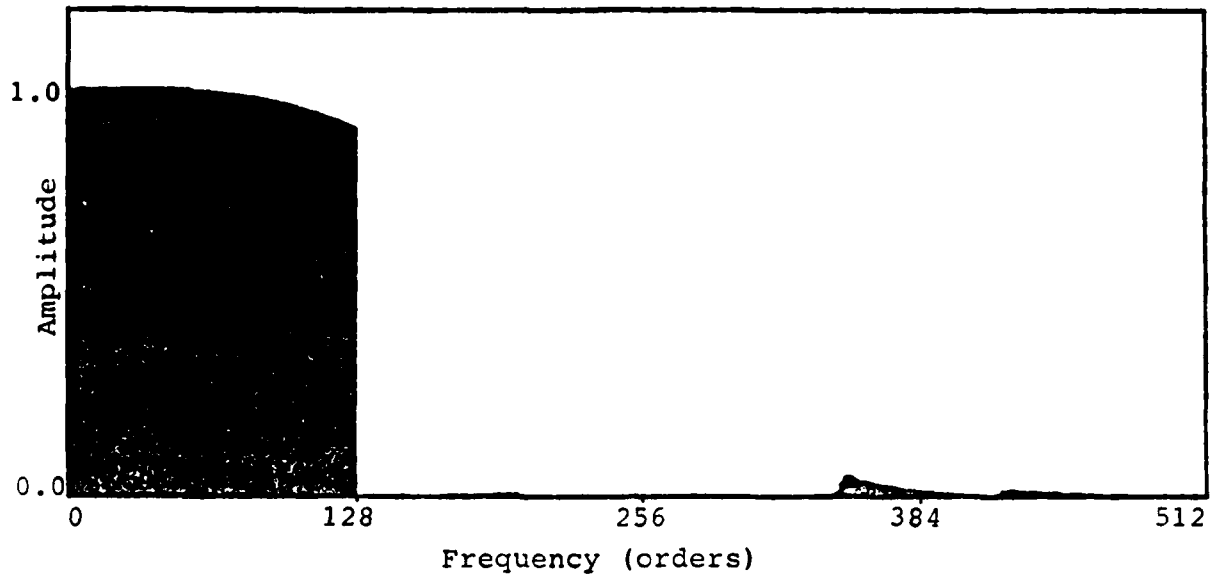

FIG. 9 AMPLITUDE SPECTRUM AFTER CUBIC INTERPOLATION OF TEST SIGNAL 1 AVERAGE

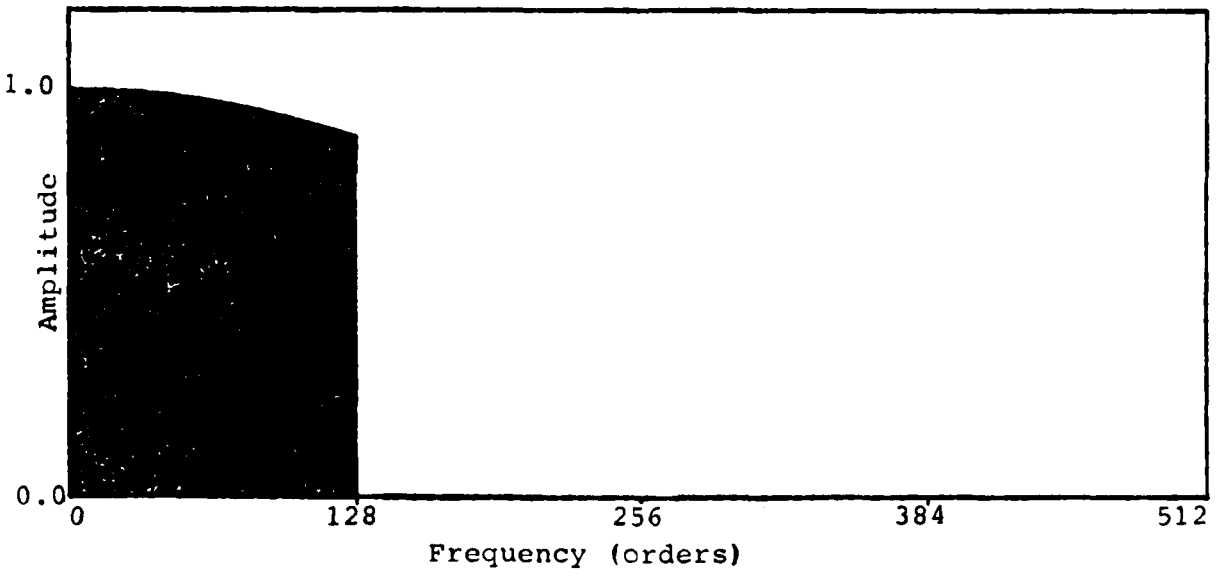

FIG. 10 AMPLITUDE SPECTRUM AFTER SAMPLE AND HOLD INTERPOLATION OF TEST SIGNAL 128 AVERAGES

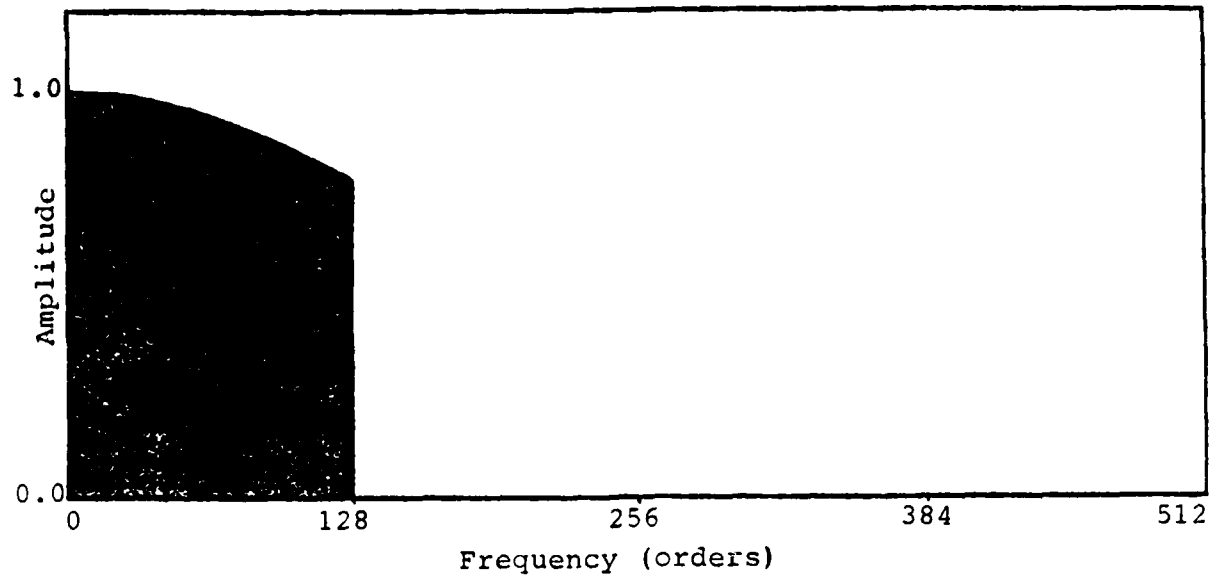

FIG. 11 AMPLITUDE SPECTRUM AFTER LINEAR INTERPOLATION OF TEST SIGNAL 128 AVERAGES

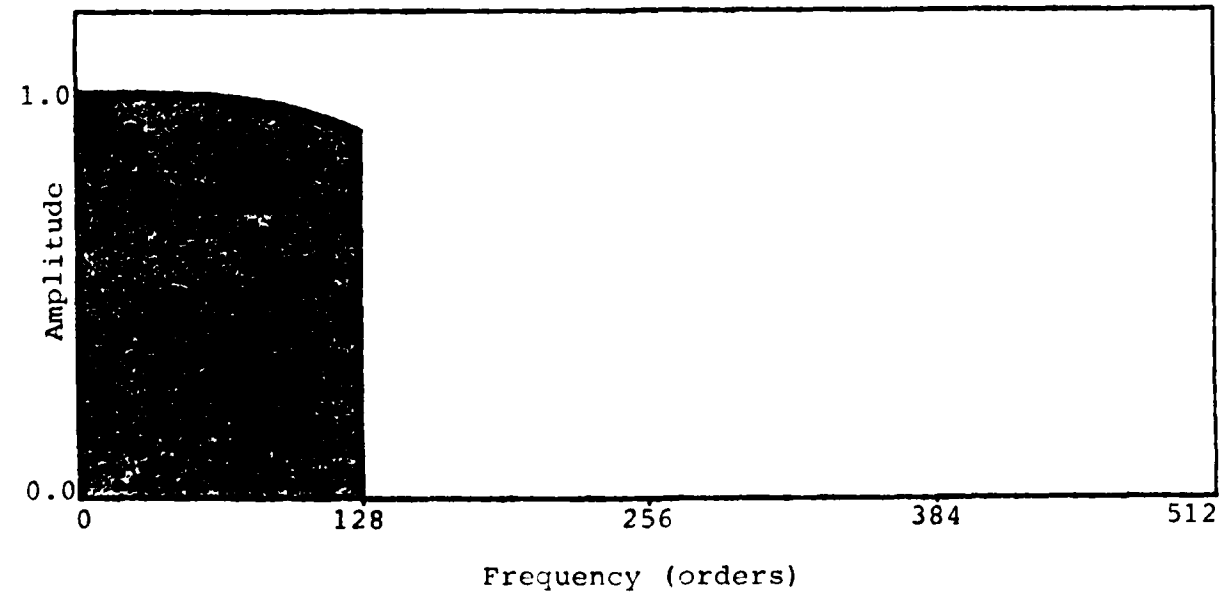

FIG. 12 AMPLITUDE SPECTRUM AFTER CUBIC INTERPOLATION OF TEST SIGNAL 128 AVERAGES

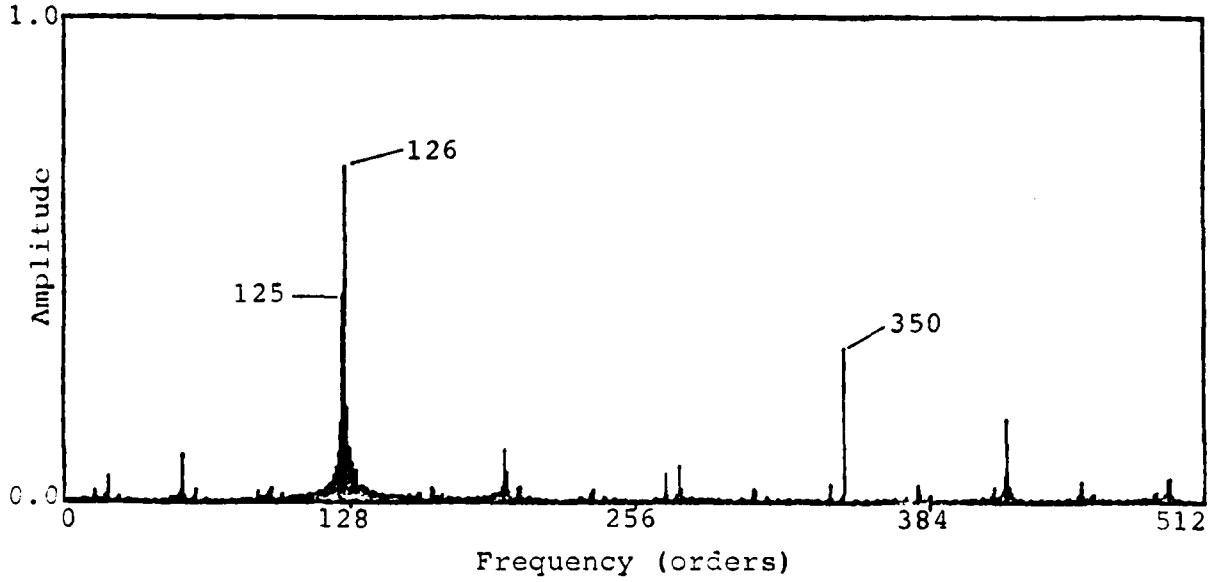

FIG. 13 AMPLITUDE SPECTRUM AFTER SAMPLE AND HOLD INTERPOLATION OF TEST SIGNAL 1 AVERAGE

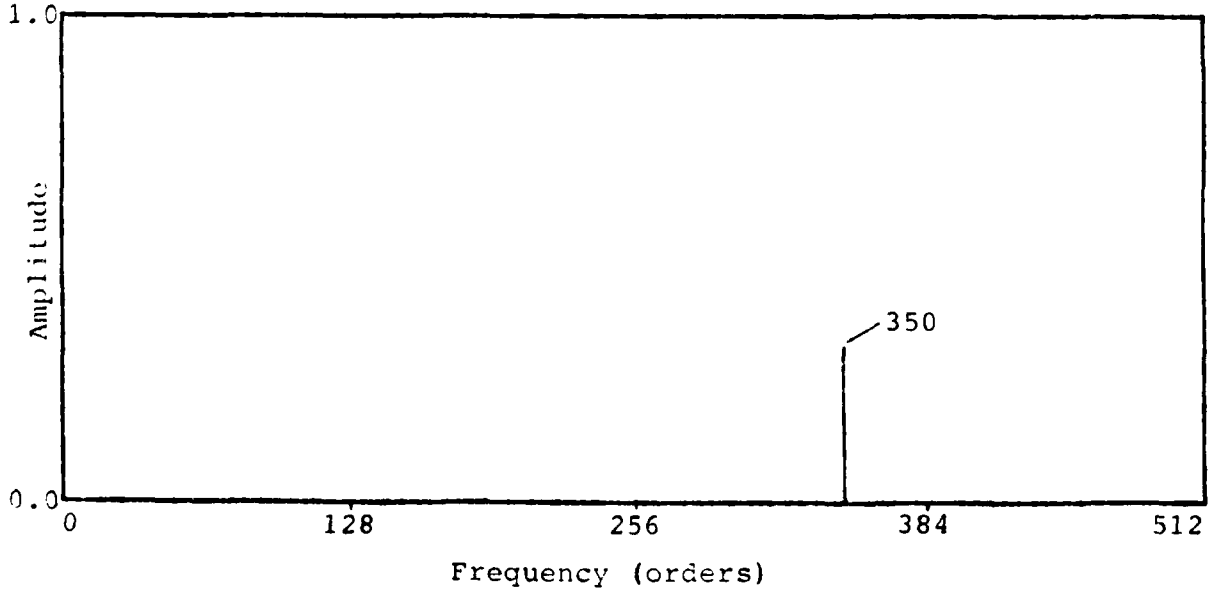

FIG. 14 AMPLITUDE SPECTRUM AFTER SAMPLE AND HOLD INTERPOLATION OF TEST SIGNAL 128 AVERAGES

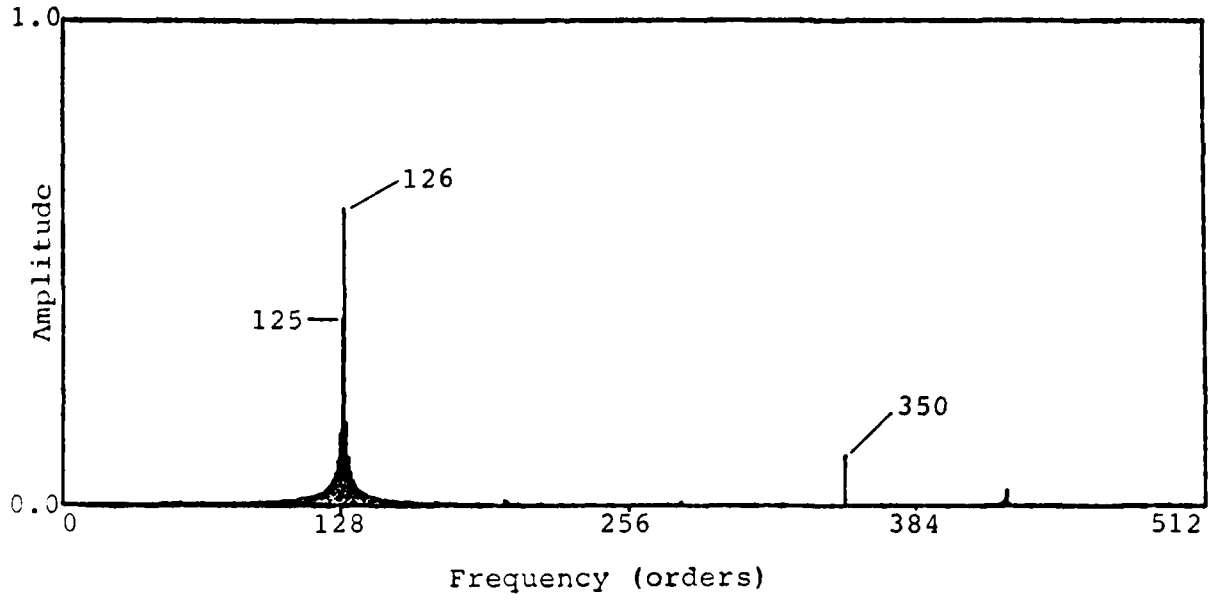

FIG. 15 AMPLITUDE SPECTRUM AFTER LINEAR INTERPOLATION OF TEST SIGNAL 1 AVERAGE

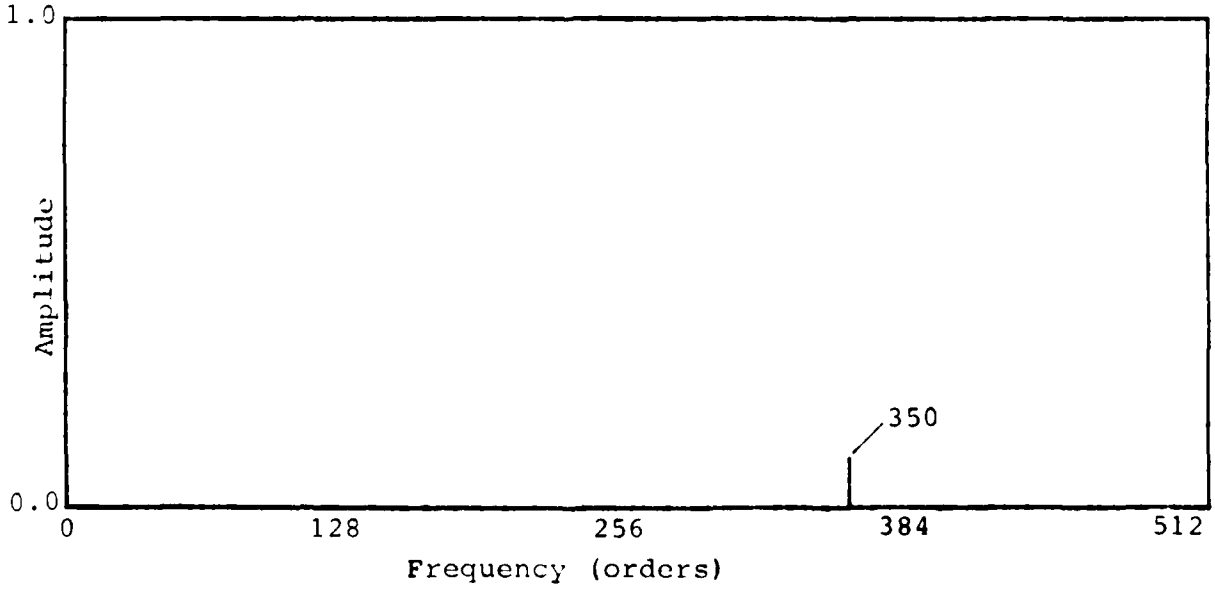

FIG. 16 AMPLITUDE SPECTRUM AFTER LINEAR INTERPOLATION OF TEST SIGNAL 128 AVERAGES

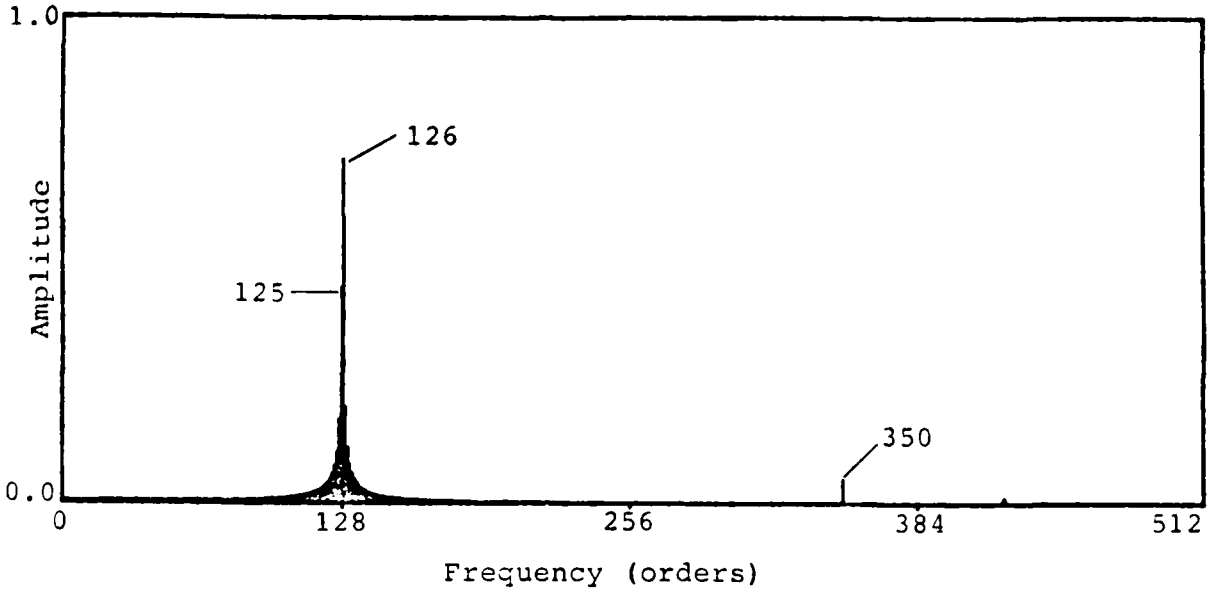

FIG. 17 AMPLITUDE SPECTRUM AFTER CUBIC INTERPOLATION OF TEST SIGNAL 1 AVERAGE

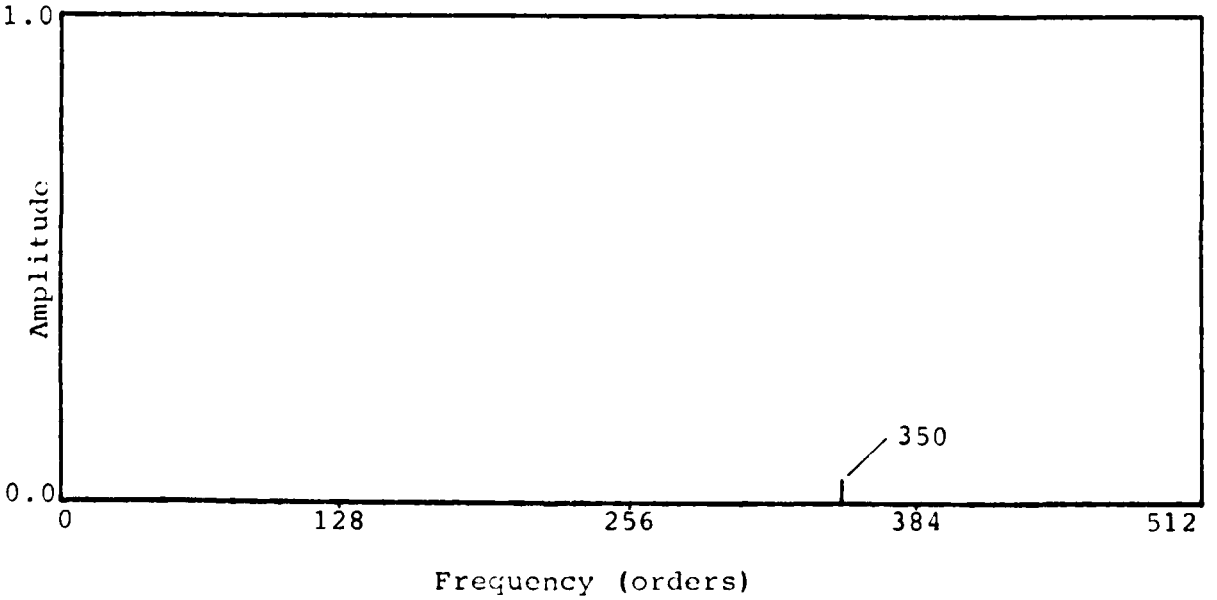

FIG. 18 AMPLITUDE SPECTRUM AFTER CUBIC INTERPOLATION OF TEST SIGNAL 128 AVERAGES

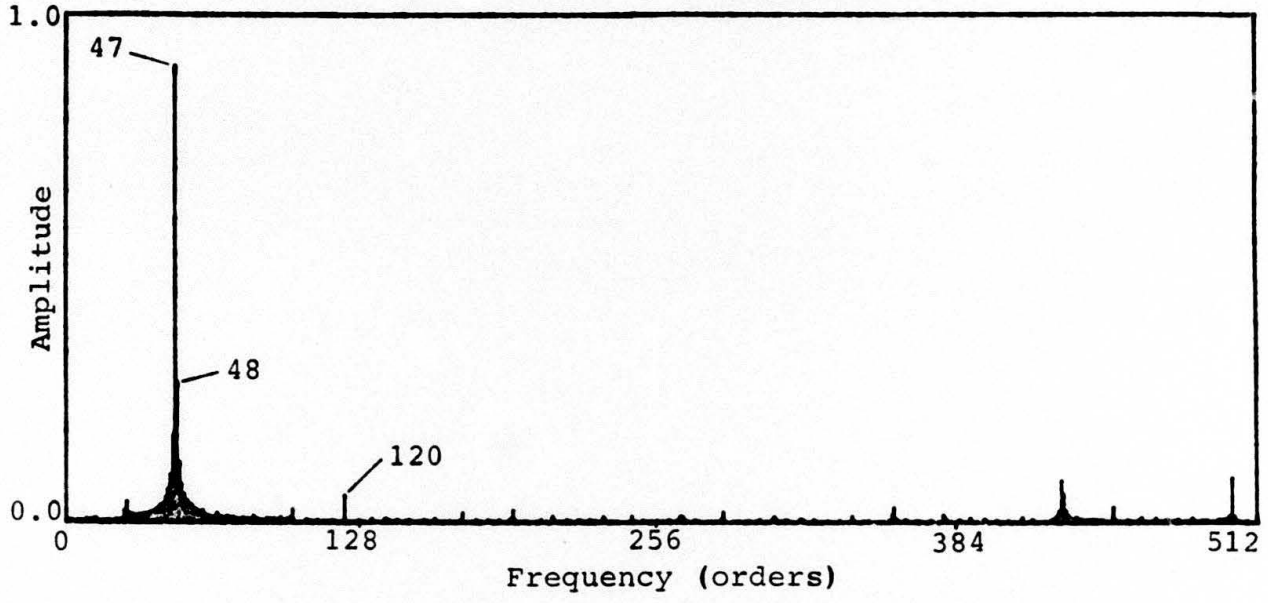

FIG. 19 AMPLITUDE SPECTRUM AFTER SAMPLE AND HOLD INTERPOLATION OF TEST SIGNAL 1 AVERAGE

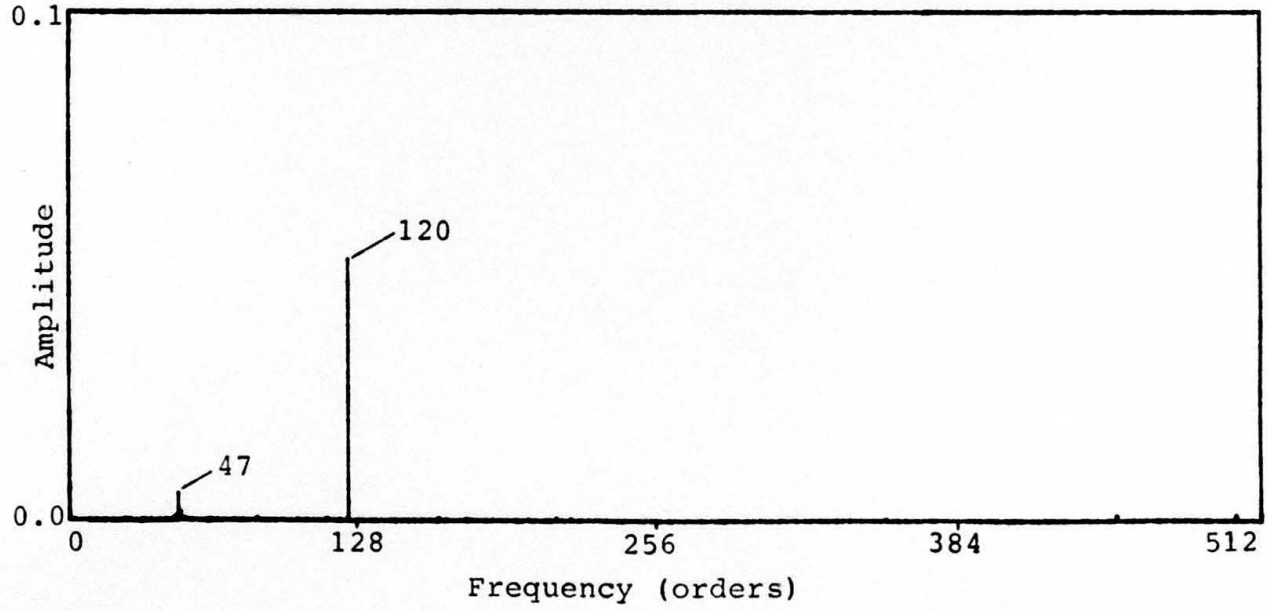

FIG. 20 AMPLITUDE SPECTRUM AFTER SAMPLE AND HOLD INTERPOLATION OF TEST SIGNAL 128 AVERAGES

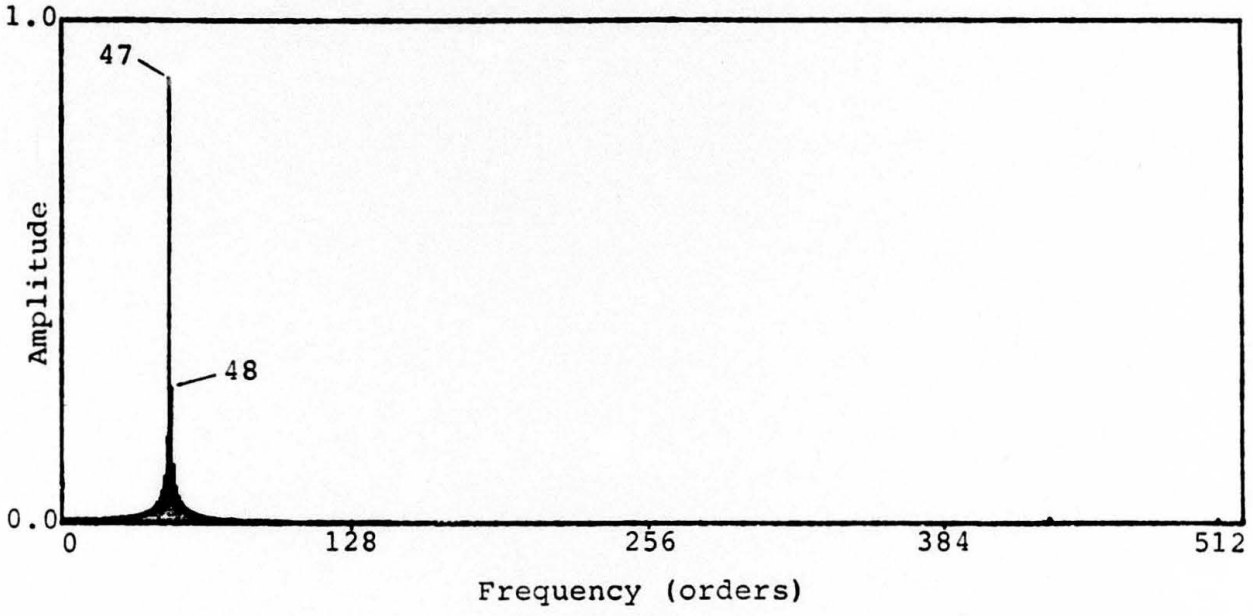

FIG. 21 AMPLITUDE SPECTRUM AFTER LINEAR INTERPOLATION OF TEST SIGNAL 1 AVERAGE

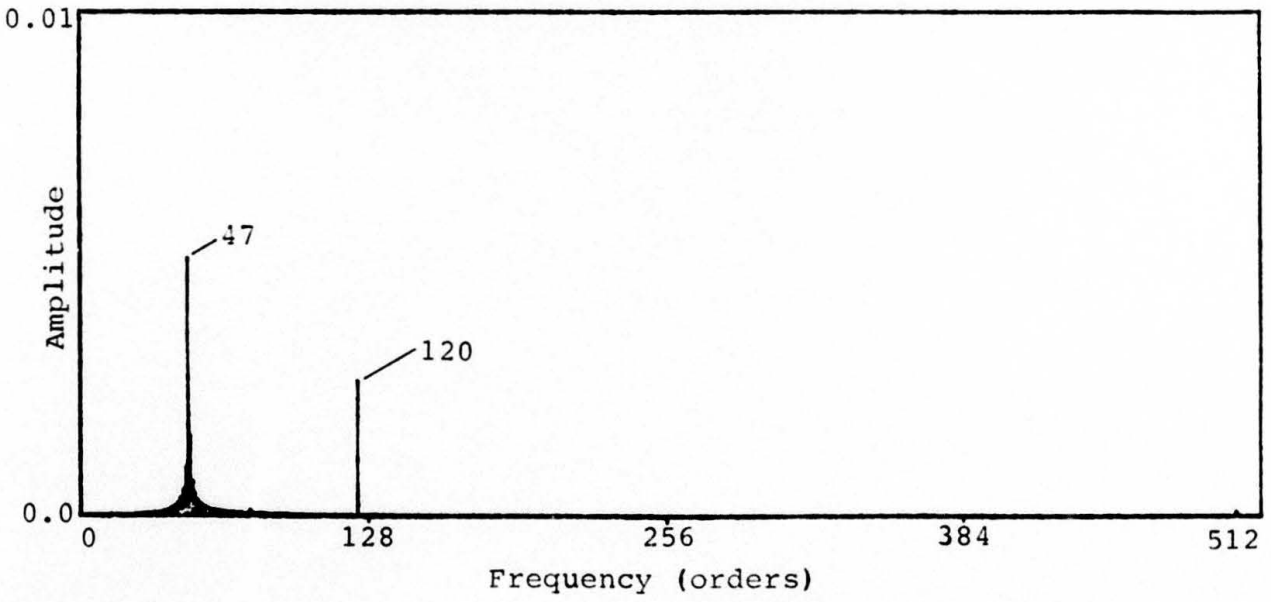

FIG. 22 AMPLITUDE SPECTRUM AFTER LINEAR INTERPOLATION OF TEST SIGNAL 128 AVERAGES

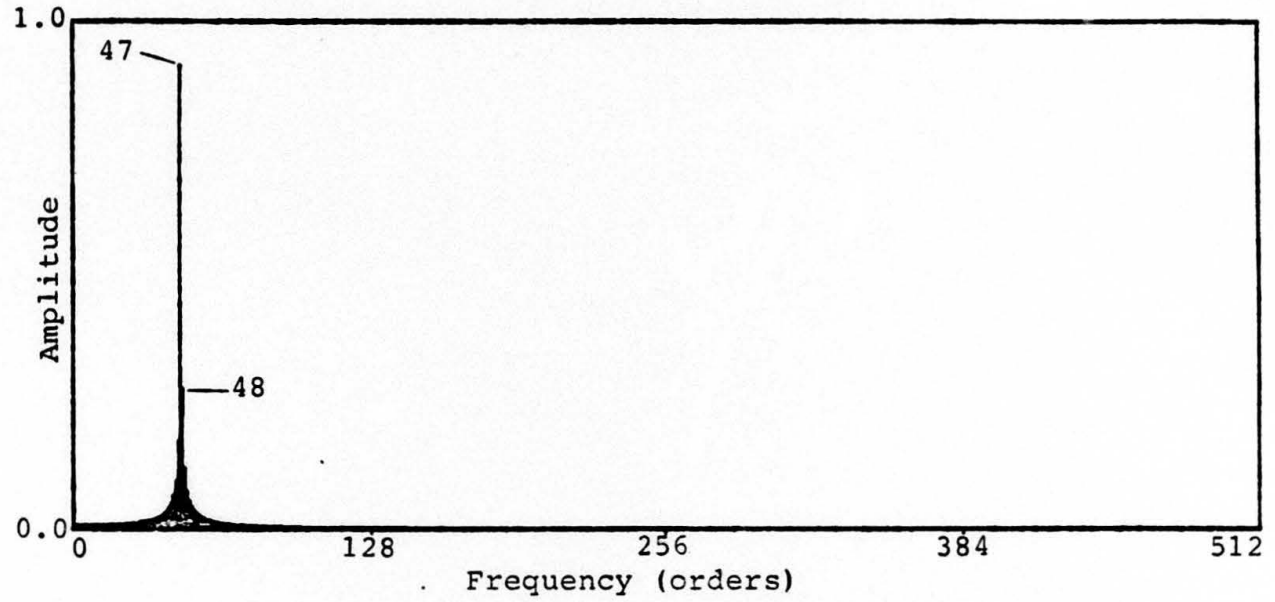

FIG. 23 AMPLITUDE SPECTRUM AFTER CUBIC INTERPOLATION OF TEST SIGNAL 1 AVERAGE

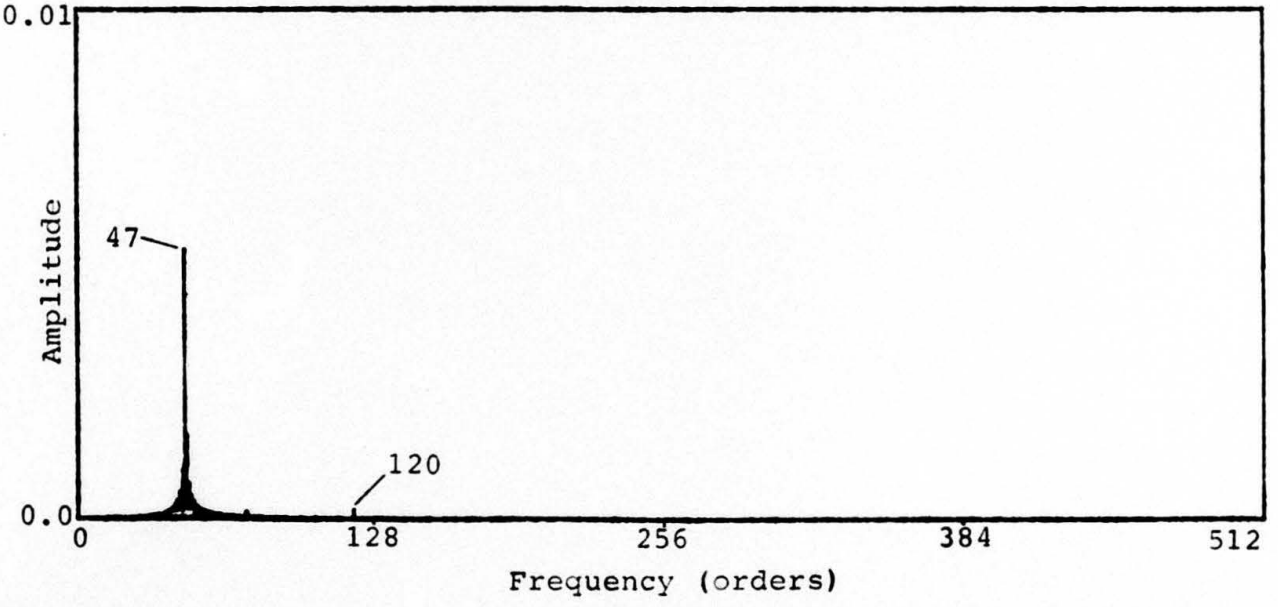

FIG. 24 AMPLITUDE SPECTRUM AFTER CUBIC INTERPOLATION OF TEST SIGNAL 128 AVERAGES

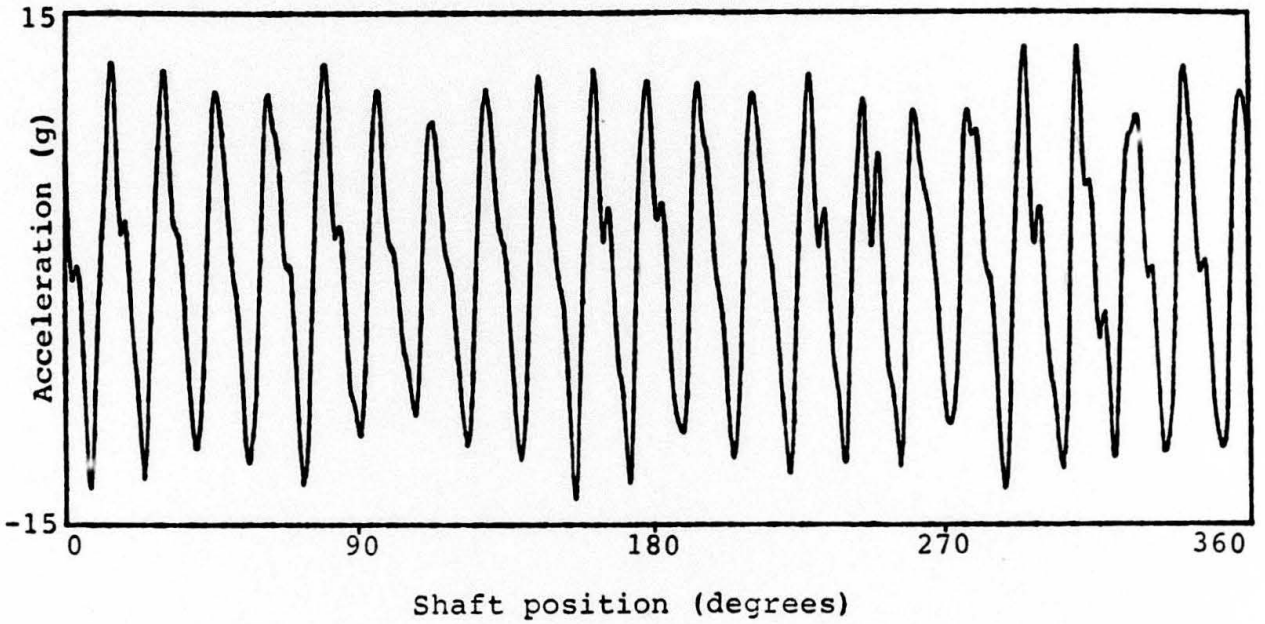

FIG. 25 TIME DOMAIN AVERAGE OF WESSEX INPUT PINION VIBRATION USING SAMPLE AND HOLD INTERPOLATION

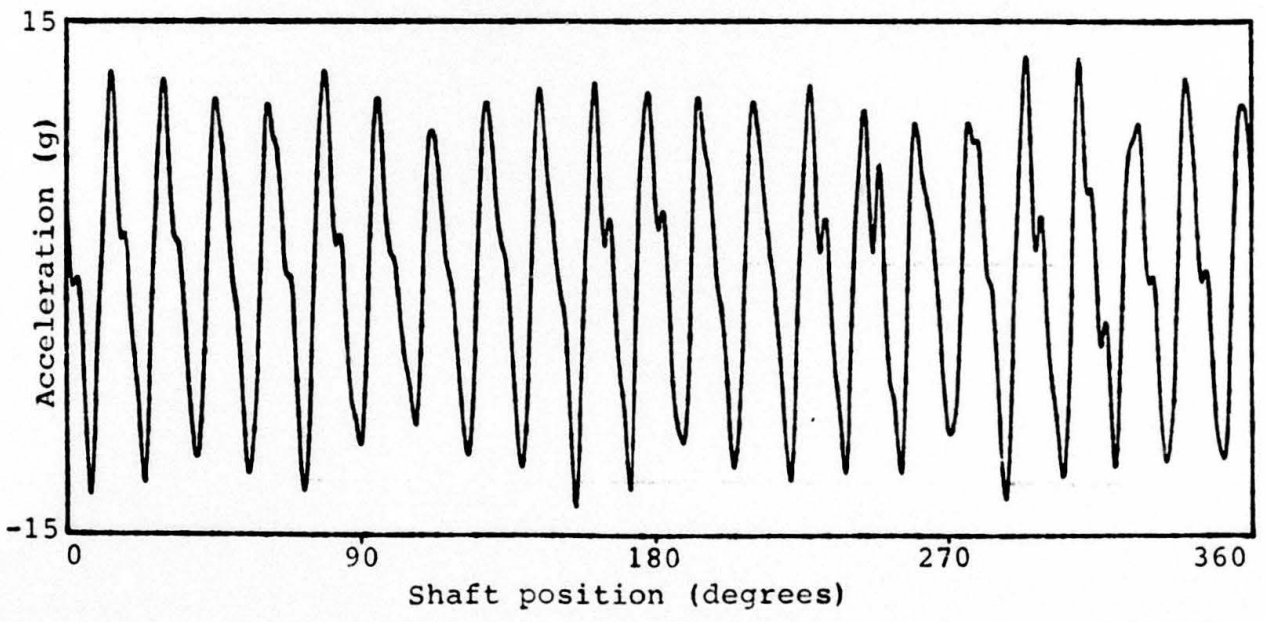

FIG. 26 TIME DOMAIN AVERAGE OF WESSEX INPUT PINION VIBRATION USING LINEAR INTERPOLATION

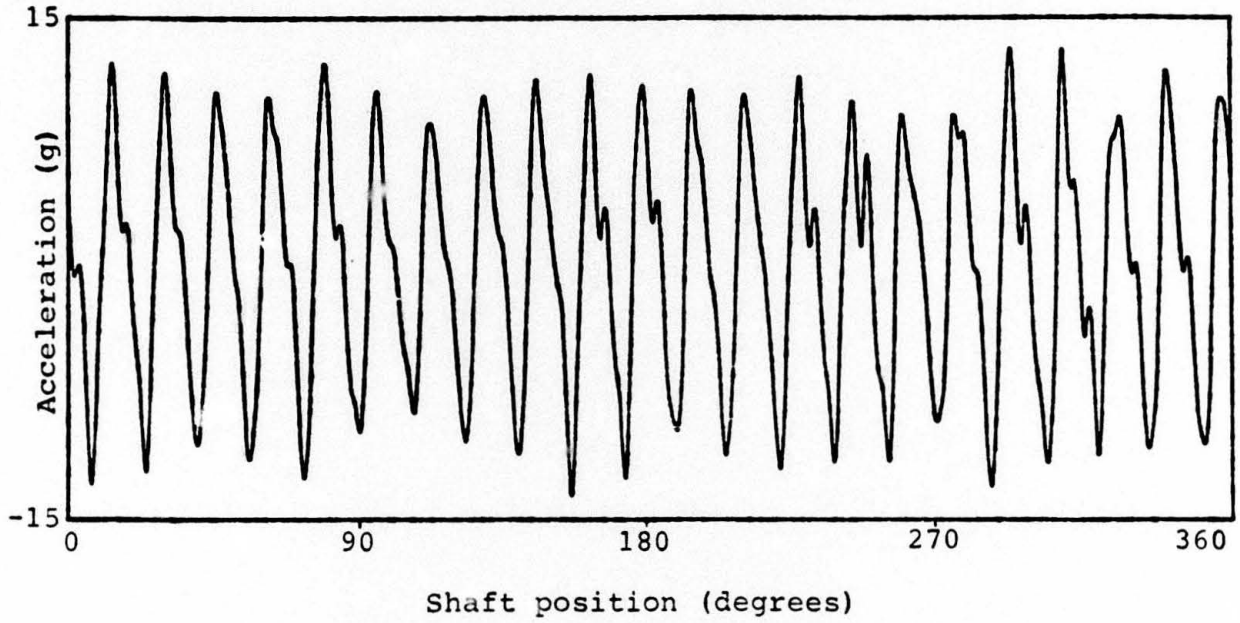

FIG. 27 TIME DOMAIN AVERAGE OF WESSEX INPUT PINION VIBRATION USING CUBIC INTERPOLATION

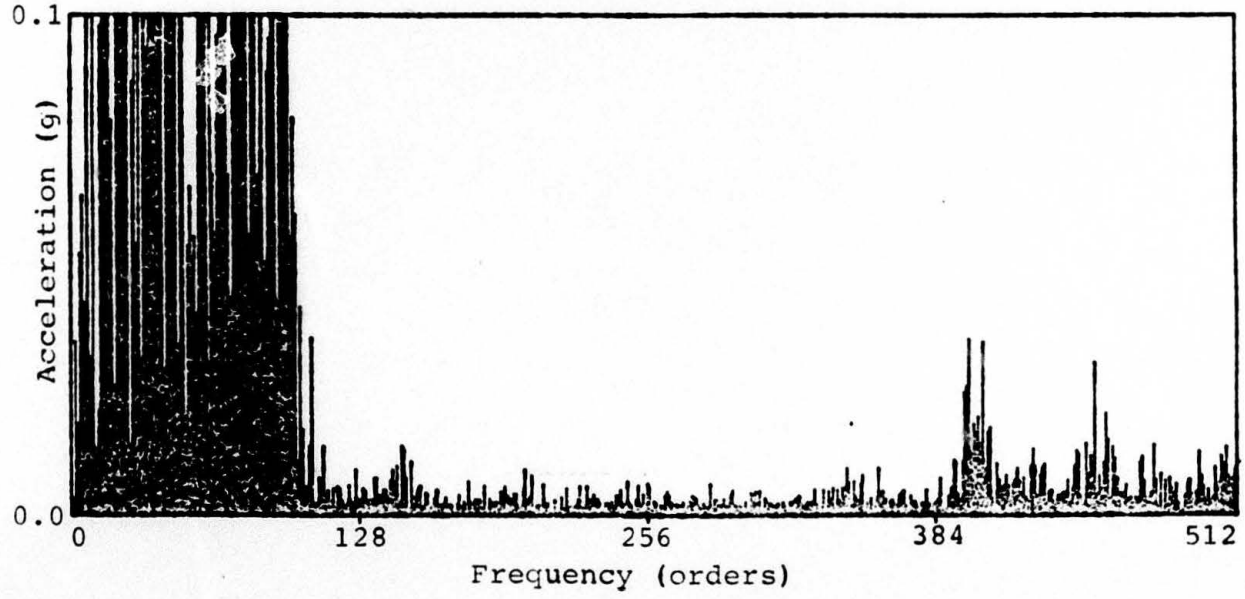

FIG. 28 AMPLITUDE SPECTRUM OF TIME DOMAIN AVERAGE OF WESSEX INPUT PINION VIBRATION USING SAMPLE AND HOLD INTERPOLATION

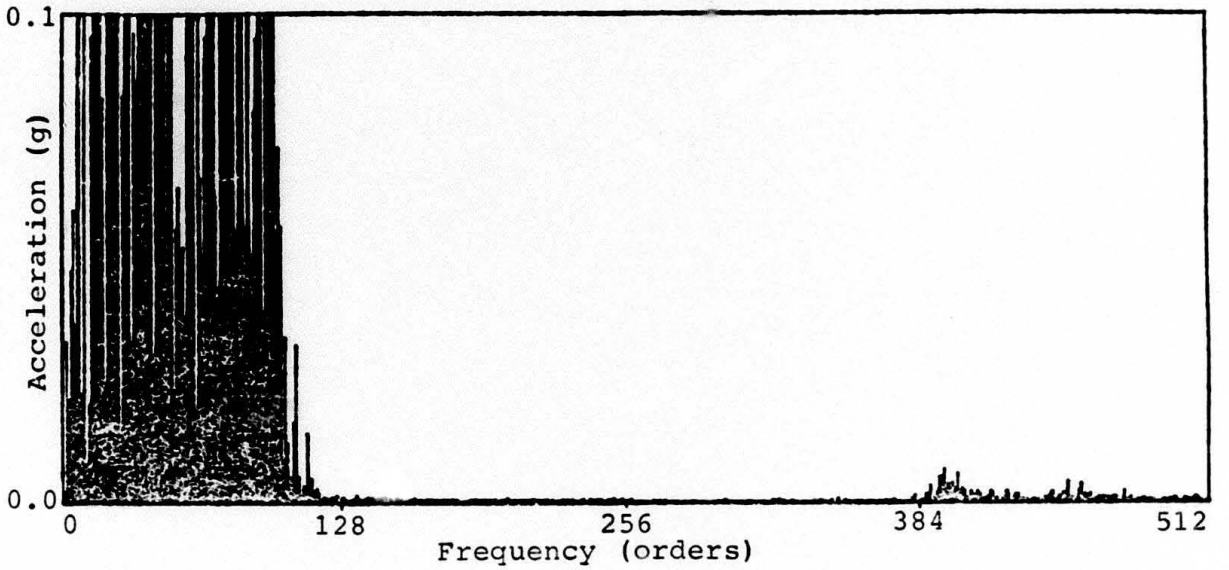

FIG. 29 AMPLITUDE SPECTRUM OF TIME DOMAIN AVERAGE OF WESSEX INPUT PINION VIBRATION USING LINEAR INTERPOLATION

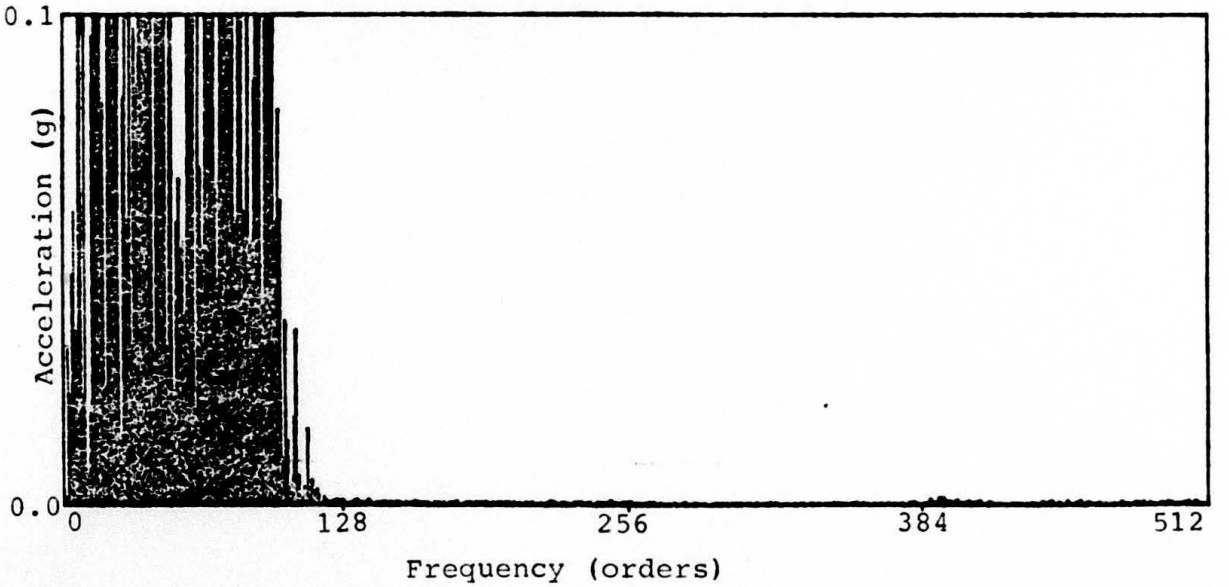

FIG. 30 AMPLITUDE SPECTRUM OF TIME DOMAIN AVERAGE OF WESSEX INPUT PINION VIBRATION USING CUBIC INTERPOLATION

DISTRIBUTION

AUSTRALIA

Department of Defence

Defence Central

Chief Defence Scientist
Deputy Chief Defence Scientist (shared copy)
Superintendent, Science and Program Administration (shared copy)
Controller, External Relations, Projects and
Analytical Studies (shared copy)
Counsellor, Defence Science, (London) (Doc Data Sheet Only)
Counsellor, Defence Science, (Washington) (Doc Data Sheet Only)
Defence Science Representative (Bangkok)
Defence Central Library
Document Exchange Centre, DISB (18 copies)
Joint Intelligence Organisation
Librarian H Block, Victoria Barracks, Melbourne
Director General - Army Development (NSO) (4 copies)

Aeronautical Research Laboratories

Director
Library
Superintendent - Aero Propulsion
Divisional File - Aero Propulsion
Author: P.D. McFadden

Materials Research Laboratories

Director/Library

Defence Research Centre

Library

Navy Office

Navy Scientific Adviser
Aircraft Maintenance and Flight Trials Unit
Director of Naval Aircraft Engineering
Director of Naval Air Warfare
Superintendent, Aircraft Maintenance and Repair

Army Office

Scientific Adviser - Army
Engineering Development Establishment, Library
Royal Military College Library

Air Force Office

Air Force Scientific Adviser
Aircraft Research and Development Unit
Scientific Flight Group
Library
Technical Division Library

Government Aircraft Factories

Library

Department of Aviation

Library
Flight Standards Division

Statutory and State Authorities and Industry

Hawker de Havilland Aust. Pty Ltd, Bankstown, Library
Hawker de Havilland Aust. Pty Ltd, Victoria, Library

Universities and Colleges

Adelaide
Barr Smith Library

Flinders
Library

La Trobe
Library

Melbourne
Engineering Library

Monash
Hargrave Library

Newcastle
Library

Sydney
Engineering Library

NSW
Physical Sciences Library
Library, Australian Defence Force Academy

Queensland
Library

Tasmania
Engineering Library

Western Australia
Library

RMIT
Library

UNITED KINGDOM
Naval Aircraft Materials Laboratory
Library

SPARES (10 copies)
TOTAL (75 copies)

Department of Defence

DOCUMENT CONTROL DATA

AD-A182 572

1.a. AR No	1.b. Establishment No	2. Document Date	3. Task No
AR-004-488	ARL-AERO-PROP-TM-437	SEPTEMBER 1986	DST 86/039

4. Title	5. Security	6. No Pages	7. No Refs
INTERPOLATION TECHNIQUES FOR THE TIME DOMAIN AVERAGING OF VIBRATION DATA WITH APPLICATION TO HELICOPTER GEARBOX MONITORING	a. document: UNCLASSIFIED b. title: U c. abstract: U	15	6

8. Author(s)	9. Downgrading Instructions
P.D. McFadden	

10. Corporate Author and Address	11. Authority (as appropriate) a.Sponsor b.Security c.Downgrading d.Approval
Aeronautical Research Laboratories P.O. Box 4331, MELBOURNE, VIC. 3001	

12. Secondary Distribution (of this document)

Approved for public release.

Overseas enquirers outside stated limitations should be referred through ASDIS, Defence Information Services Branch, Department of Defence, Campbell Park, CANBERRA ACT 2601

13.a. This document may be ANNOUNCED in catalogues and awareness services available to ...

No limitations.

13.b. Citation for other purposes (ie casual announcement) may be ~~(unlimited)~~ unrestricted ~~(or as for 13a).~~

14. Descriptions		15. COSATI Group
Vibration Gear boxes, Helicopters,	Signal averaging, Condition monitoring, Australia.	01030 13090 14020

16. Abstract

Interpolation techniques provide an alternative to the phase-locked frequency multiplier for the calculation of the time domain average of a vibration signal. Higher order interpolation techniques produce flatter passbands and lower sidelobes in the stopband but require longer calculation times. Aliasing errors are introduced into the result by replication of the sidelobes during interpolation. In general, the errors are attenuated by time domain averaging, but under some conditions may be passed without attenuation. Keywords:

PF 65

A

This paper is to be used to record information which is required by the Establishment for its own use but which will not be added to the DISTIS data base unless specifically requested.

16. Abstract (contd)

17. Imprint

Aeronautical Research Laboratories, Melbourne

18. Document Series and Number	19. Cost Code	20. Type of Report and Period Covered
AERO-PROPULSION TECHNICAL MEMORANDUM 437	41 3146	

21. Computer Programs Used

22. Establishment File Ref(s)